

STUDIES ON THERMAL AND MATERIAL

TRANSFER IN TURBULENT FLOW

- I. Problems in Turbulent Heat Transfer
- II. An Attempt to Measure the Eddy Diffusivity in Uniform Turbulent Flow

Thesis by

Rodman Jenkins

In Partial Fulfillment of the
Requirements for the degree of
Doctor of Philosophy

California Institute of Technology
Pasadena, California

1949

ACKNOWLEDGMENT

The encouragement of Professor B. H. Sage has been of great assistance throughout the course of this work. His initiative is primarily responsible for the accomplishments of the heat transfer project in the Chemical Engineering Laboratory.

Experimental measurements made by Franklin Page, S. D. Cavers, and other members of this project have been used in this thesis. Sincere thanks is expressed to these students, and to B. H. Sage for permission to use this data.

The advice and assistance of H. H. Reamer in the experimental work described here was particularly helpful.

ABSTRACT

I.

A method of correlating experimental values of the eddy viscosity in turbulent flow inside tubes and rectangular channels is described. A procedure for predicting the influence of physical properties on the ratio of the eddy conductivity to the eddy viscosity is presented. The values of the eddy conductivity obtained in this manner have been used to predict rates of heat transfer inside tubes which check well with experimental values.

II.

A study of the evaporation of iodoform containing radioactive iodine is described. An attempt was made to measure the eddy diffusivity in a turbulent air stream through this study. The use of radioactive materials for measuring small concentrations of vapors in gaseous mixtures was investigated. No measurements of concentrations in turbulent air flow, and consequently, no values of the eddy diffusivity were obtained.

TABLE OF CONTENTS

	Page
Introduction	1
Part I. Problems in Turbulent	5
Heat Transfer	
Measurement and Correlation of.	6
the Eddy Conductivity and Eddy	
Viscosity in Uniform Flow	
Prediction of the Effect of Fluid	12
Properties on the Ratio of the Eddy	
Conductivity to the Eddy Viscosity	
Prediction of Overall Heat Transfer	17
Rates Inside Circular Conduits	
Momentum and Thermal Transfer in	32
Non-uniform Turbulent Flow	
Part II. An Attempt to Measure the Eddy	
Diffusivity in Uniform Turbulent Flow	59
Radiation Measurement.	60
The Heat Transfer Apparatus	72
Portable Analysis Unit	73
Preparation and Deposition of	
Iodoform	76
Appendix I	100
Appendix II	103

INTRODUCTION

The fields of heat transfer, momentum transfer, and material transfer are of great importance to many industries. Many millions of dollars are invested every year in equipment for transporting, heating or cooling, and changing the composition of various fluids. When construction of such apparatus is based on rational design, it is almost invariably the result of empirical correlation.

The Chemical Engineering Laboratory of the California Institute of Technology is now undertaking a long range investigation of the fundamental mechanism of these transfer processes. The work presented in this paper covers two parts of this study. Means of using the experimental information on heat transfer obtained in this project to predict the performance of industrial equipment are given. Secondly, a method investigated for the experimental study of eddy diffusion, which did not yield successful results, is described.

The development of a fundamental approach to problems in heat and mass transfer originated with the work of Osbourne Reynolds, (1)*, in 1874. The papers of L. Prandtl, (2), and Th. von Karman, (3), are outstanding among the many that have appeared in subsequent years. The theories

* References given in this section are tabulated in Part I.

of these writers are based on the use of three quantities, ϵ_v , the eddy viscosity, ϵ_c , the eddy conductivity, and ϵ_D , the eddy diffusivity. These variables are defined by the equations

$$\tau/\rho = (\epsilon_v + \nu) \frac{du}{dy}$$

$$\frac{\dot{Q}}{c_p \sigma} = (\epsilon_c + K) \frac{dt}{dy}$$

$$M = (\epsilon_D + D) \frac{dc}{dy}$$

Reynolds originally proposed that all these eddy quantities are equal. This hypothesis is supported by Prandtl's momentum transfer theory, (4), but is not in agreement with the vorticity transfer theory of G. I. Taylor, (5). Experiments made in the Chemical Engineering Laboratory at the California Institute have shown that ϵ_c and ϵ_v are equal in uniform air streams.

In order to predict the changes in temperature that will occur under specified physical conditions, it is necessary to know the value of ϵ_c as a function of position in the stream under consideration. Karman and Prandtl have accomplished this assuming the equality $\epsilon_c = \epsilon_v$ and obtain-

ing ϵ_v from velocity distribution equations, (3), (6).

In the present work, a new method of correlating experimental values of ϵ_v directly has been presented. A procedure for predicting the influence of fluid physical properties on the ratio $\frac{\epsilon_c}{\epsilon_v}$ is given. The values of ϵ_c obtained in this way have been utilized to predict rates of overall heat transfer inside tubes which agree satisfactorily with experimental determinations. Two new procedures for predicting temperature distributions and heat transfer rates from a knowledge of ϵ_c are presented.

The work on eddy diffusion which was attempted was a study of the evaporation of iodofrom containing radioactive iodine - 131 into a turbulent air stream. The objective of this project was to provide a means of measuring concentrations in turbulent air streams, so that values of ϵ_D could be obtained. The evaporation of material from a solid surface was chosen in order to avoid difficulties found by previous investigators, (7), (8), (9). These latter studies consisted of evaporation from liquid surfaces, and injection of a gas into another gas stream of different composition. Considerable undesirable disturbance of the flow resulted from both of these techniques.

In the experiments which the author tried, the air channel used was that in the heat transfer apparatus of the Chemical Engineering Laboratory of the California Institute.

This apparatus is described in detail by Mason, (10). The air flows between two copper plates $3/4$ inch apart, $12\ 3/8$ inches wide, and 13 feet in length. The iodoform was sprayed onto a fixed area of the lower plate, and air samples were taken from the region above the sprayed area. It was hoped to determine the concentration of iodoform vapor relative to saturation by measuring the intensity of the radiation from the air samples and comparing this intensity with that of the saturated vapor.

No experimental data on the vapor concentration were obtained. The radiation emitted by the air samples was found to be too weak to measure. It was concluded, that while the iodoform disappeared from the plate, it blew away, and did not evaporate.

Part I

Problems in Turbulent Heat Transfer

MEASUREMENT AND CORRELATION OF THE EDDY CONDUCTIVITY
AND EDDY VISCOSITY IN UNIFORM FLOW

Although velocity distributions in turbulently flowing streams have been measured by quite a number of investigators in this century, no adequate general method of predicting eddy viscosities is now in the literature. Usually, attention has been given to approximate correlation of the velocity data itself. The eddy viscosity, which is a much more sensitive variable, has received little consideration.

Values of the eddy viscosity and eddy conductivity obtained by the transfer research program of this department have been used in the present work to provide a direct correlation of these quantities.

The experimental measurements of eddy quantities have been made on the heat transfer research apparatus in this department. This equipment is described in full by Corcoran, (27). In brief, it consists of two parallel copper plates, 1 foot wide, 13 feet long, with a $3/4$ inch air channel in between them. These plates are independently maintained at any desired temperature by means of oil baths above the upper plate and below the lower plate. Heat transfer experiments are made by maintaining the upper plate at a higher temperature than the lower plate and measuring

the temperature distribution in the air channel. Values of the eddy viscosity are obtained from velocity determinations obtained at the same time as the temperature data.

The results of the most accurate measurements in uniform flow obtained thus far are shown in Figure 1. It is evident that the values of the eddy viscosity are identical with the values of the eddy conductivity within the experimental uncertainty.

Further inspection of Figure 1 points out the characteristic shape of the curves, and the increase of the values with the velocity of the fluid. The slight asymmetry of the curves is probable not due to the temperature variation in the air stream. It is also seen in experiments made with both plates at the same temperature.

The work of Nikuradse, (6), and von Karman, (3), has resulted in specific equations for the eddy viscosity. These equations predict the decrease of this quantity to zero at the centerline of pipes and channels, which is not observed here. The expression applying to the main part of the flowing stream, called the turbulent core, is, in dimensionless form,

$$\frac{\epsilon_v + \nu}{\nu} = \frac{(1 - 2y/y_0)^{2.5}}{2.5} Re \sqrt{f/2} \quad (1)$$

If the product of the Reynold's number and $\sqrt{f/2}$

are transposed to the left-hand side of equation (1), we obtain

$$\left(\frac{\epsilon_v}{\nu} + 1\right) \frac{1}{Re \sqrt{f/2}} = \left(1 - 2y/y_0\right) \frac{y}{y_0} \quad (2)$$

We note that here the group $\left(\frac{\epsilon_v}{\nu} + 1\right) \frac{1}{Re \sqrt{f/2}}$ is expressed as a universal function of y/y_0 .

The data of this laboratory have been expressed as the function $\frac{(\epsilon_v/\nu + 1)}{Re \sqrt{f/2}}$ and plotted versus y/y_0 in Figure 2. The universal curve of Nikuradse and another curve used later in the present investigation are also shown. Values of both the eddy viscosity and eddy conductivity have been used, since these variables have been found essentially equal throughout any one experiment.

Inspection of the points in Figure 2 shows that there is a possibility of securing a general correlation of the data in this manner, although more data must be compared before this proposition can be adequately tested. It seems likely that, at least over a limited range, eddy viscosity values will fall on a single curve when plotted as in Figure 2. In any event, a closely similar family ^{OF} curves changing slowly with Reynold's number would at least be expected. The writer believes that the treatment of eddy viscosity data in this form clarifies the influence of the physical properties of the fluid to a considerable degree.

It should be pointed out that the deviation of the two sets of data on the right side of Figure 2 does not arise in the method of correlation. Both curves in Figure 1 are seen to be unsymmetrical, the high side being different in the two cases. In an experiment made with no heat transfer through the air stream at a nominal velocity of 30 ft/sec, the eddy viscosities found were 30% above those in the lower curve of Figure 1. This supports the conclusion that small changes in the apparatus between experiments may be responsible for the lack of correlation in Figure 2. Earlier, less precise data on the eddy conductivity determined on this apparatus have been omitted for this reason.

If future work verifies the general correlation of eddy viscosity data by means of a single curve in the coordinates of Figure 2, a universal velocity distribution may then be obtained from this curve.

Let us represent this eddy viscosity correlation by the equation

$$\frac{(\epsilon_v + \nu)}{\nu} = Re \sqrt{f/2} f_1 \left[\frac{r}{r_0} \right] \quad (3)$$

The definition of the eddy viscosity may be written

$$\epsilon_v + \nu = \left(\frac{\tau}{\rho} \right) \frac{1}{\left(\frac{du}{dr} \right)} \quad (4)$$

Between parallel plates, or inside a circular conduit, the shear force is expressed by

$$\tau = \tau_0 \frac{2r}{y_0} \quad (5)$$

Combining these expressions, we find

$$\left(\frac{2r}{y_0}\right) \left(\frac{\tau_0}{\rho}\right) \frac{1}{v \left(\frac{du}{dr}\right)} = Re \sqrt{f/2} f_1 \left[\frac{r}{y_0}\right] \quad (6)$$

It may be shown that

$$\sqrt{\frac{\tau_0}{\rho}} = V \sqrt{f/2}$$

Introducing this equality into equation (6),

$$\left(\frac{2r}{y_0}\right) V y_0 \sqrt{f/2} \frac{1}{v \left(\frac{d \frac{u}{V}}{d \frac{r}{y_0}}\right)} = Re f_1 \left[\frac{r}{y_0}\right] \quad (7)$$

Since $\frac{y_0 V}{\nu} = Re$, and using Prandtl's equality again, we find

$$\frac{d u^+}{d \frac{r}{y_0}} = \frac{\frac{2r}{y_0}}{f_1 \left[\frac{r}{y_0}\right]} \quad (8)$$

Indicating the integration of equation (8), we obtain our universal velocity distribution expression

$$u^+ = \int \frac{\left(\frac{r}{y_0}\right) d\left(\frac{r}{y_0}\right)}{f_1 \left[\frac{r}{y_0}\right]} + \text{constant} \quad (9)$$

By choosing the appropriate value of the constant of integration in equation (9), this expression may be used for any region in the turbulent stream in which the proposed eddy viscosity correlation is valid. In other words, if equation (3) represents the eddy viscosity satisfactorily only in the central portion of the fluid stream, the integration in equation (9) may be limited to this region, and the constant of integration (which may be a function of Re) evaluated at the boundary of this area.

PREDICTION OF THE EFFECT OF FLUID PROPERTIES ON THE RATIO
OF THE EDDY CONDUCTIVITY TO THE EDDY VISCOSITY

The experimental results discussed in the preceding section show clearly the equality of these eddy quantities in uniformly flowing air streams. Since many of the more important applications of eddy conductivity studies are in the flow of other materials, the extension of this data to such cases is of considerable interest.

Much work in the literature, (3), (11), (12), (13), is based on the tacit assumption that $\epsilon_c = \epsilon_v$, regardless of the properties of the fluid. This assumption is probably the result of considering the turbulent transfer processes to be influenced only by fluid motion. The present author believes that, particularly in less violent turbulence, transfers of momentum and energy within the eddies by means of the absolute viscosity and thermal conductivity of the fluid are quite important.

In order to make a quantitative estimate of the variation of $\frac{\epsilon_c}{\epsilon_v}$ in different media an idealized "model" has been employed to represent the actual turbulent motion. The early mixing length theory of Prandtl, (4), has been used for this purpose. This theory visualizes transfer processes in turbulence as due to the exchange of particles of fluid between regions having different mean velocities

and temperatures. That is, an "eddy" originates in one plane, moves through the fluid with constant velocity and temperature for a specific distance defined as the "mixing length", and then disintegrates, leaving its entire momentum and internal energy in the second layer.

The present treatment alters this concept only by allowing the moving particles to change their energy and momentum while in flight. This change is considered to result only from the thermal conductivity and molecular viscosity of the "eddies". Such an effect must be present; the temperature of a solid body moving through a liquid in a region of positive temperature gradient will increase.

In order to use the temperature history of an eddy to calculate ϵ_c we shall use an equation for turbulent heat transfer derived by Reynolds, (1),

$$\frac{\dot{Q}_0}{c_p \sigma} = \overline{t' v'} \quad (10)$$

If the temperature of the eddy did not change in flight, our definition of the mixing length on the previous page would give us

$$\epsilon_c = \overline{l v'} \quad (11)$$

since $t' = l \, dt/dy$. However, since t' is actually less than this amount, we have instead

$$\epsilon_c = l v' \frac{t_s - t_0}{l (dt/dy)} \quad (12)$$

In order to obtain an expression for $\frac{t_s - t_0}{l dt/dy}$, the eddies have been assumed to be spheres having a radius equal to the mixing length. The surface temperature of the particles is assumed to vary linearly with time during its movement. The interval of time between the eddy's creation and its destruction is taken as l/v' . Carslaw and Jaeger, (14), give the average temperature of the sphere under these conditions by the formula

$$t - t_0 = \frac{dt}{dy} \left\{ \frac{l^2}{15K} + \frac{6l^2}{K\pi^4} \sum_{n=1}^{\infty} \frac{1}{n^6} \left(1 - e^{-\frac{n^2 \pi^2 K}{\theta}} \right) \right\} \quad (13)$$

At the time $\theta = l/v'$, this may be combined with equation (12) to give the expression

$$\frac{\epsilon_c}{l v'} = \frac{l v'}{K} \left\{ \frac{2}{15} - \frac{12}{\pi^6} \left(\frac{l v'}{K} \right) \sum_{n=1}^{\infty} \frac{1}{n^6} \left(1 - e^{-\frac{n^2 \pi^2 K}{l v'}} \right) \right\} \quad (14)$$

The curve represented by this equation is plotted in Figure 3.

A complete analysis of the analogous effect of molecular viscosity on momentum transfer cannot be obtained directly. However, the analogy between the effects of thermal conductivity and viscosity is so close that the writer has felt justified in applying an equation corre-

sponding to (14) for calculation of the eddy viscosity. In other words, it is assumed

$$\frac{\epsilon_v}{l\nu'} = \frac{l\nu'}{K} \left\{ \frac{2}{15} - \frac{12}{\pi^6} \left(\frac{l\nu'}{\nu} \right) \sum_{n=1}^{\infty} \frac{1}{n^6} \left(1 - e^{-n^2 \pi^2 \nu / l\nu'} \right) \right\} \quad (15)$$

This procedure is supported by the recent demonstration of Batchelor, (35), that momentum transfer (or energy dissipation) in small scale turbulence is governed by viscosity in an equation analogous to that for heat conduction.

An expression giving the ratio of ϵ_c to ϵ_v explicitly is obtained from division of equation (14) by equation (15). The result is

$$\frac{\epsilon_c}{\epsilon_v} = Pr \left\{ \frac{\left[\frac{2}{15} - \frac{12}{\pi^6} \left(\frac{l\nu'}{K} \right) \sum_{n=1}^{\infty} \frac{1}{n^6} \left(1 - e^{-n^2 \pi^2 K / l\nu'} \right) \right]}{\left[\frac{2}{15} - \frac{12}{\pi^6} \left(\frac{l\nu'}{\nu} \right) \sum_{n=1}^{\infty} \frac{1}{n^6} \left(1 - e^{-n^2 \pi^2 \nu / l\nu'} \right) \right]} \right\} \quad (16)$$

Curves expressing this relationship for various values of ϵ_v/ν are shown in Figure 4.

The information shown in Figure 4 may be used in the calculation of overall heat transfer rates inside tubes, in the estimation of temperature distributions inside tubes with and without the presence of chemical reactions, and in many other ways.

However, it must be emphasized that these results are at present entirely speculative. The basic assumptions of this derivation may not be fulfilled in very weak

turbulence, i. e., where ϵ_v/ν is, say, less than unity. Consider flow near a solid wall, in the so-called "buffer layer", where flow is alternately turbulent and laminar. It seems that here, turbulent friction may be due to momentary distortion of the streamlines, and formation of vortices. The interchange of well defined elements of fluid between planes of different velocity is considered unlikely under these conditions.

The theory presented here predicts values of $\frac{\epsilon_c}{\epsilon_v}$ under conditions where no other information is available. By giving even a very rough picture of what is to be expected, it may be a useful guide for future experimental work. When ϵ_v/ν is very small and the theory is more uncertain, the effects of molecular viscosity and conductivity are largest. The approach of previous workers, (12), (13), who neglected these effects, is even more uncertain.

The experimental measurements of ϵ_c and ϵ_v made in this department in turbulent air streams do not test this theory severely. Since air has a Prandtl number of 0.74, the predicted values of ϵ_c/ϵ_v are all very close to unity, as may be seen in Figure 4. As measured, this ratio is unity within the experimental uncertainty of 10%. Since the theory predicts $\frac{\epsilon_c}{\epsilon_v} = 1$ when the effects of physical properties are negligible ($\frac{\epsilon_v}{\nu} \rightarrow \infty$), this agreement does not make a major contribution of support for this theory.

PREDICTION OF OVERALL HEAT TRANSFER RATES
INSIDE CIRCULAR CONDUITS

There have been several workers in recent years, (3), (12), (13), who have given equations for overall heat transfer obtained from assumed values of the eddy conductivity. Similar calculations have been made from the theory of the preceding section. This work is compared with experimental data, and the previous theories.

Temperature distributions in turbulent streams are governed by the partial differential equation derived in

Appendix I

$$\frac{\partial \left[r(k + \epsilon_c) \frac{\partial t}{\partial r} \right]}{\partial r} = r\mu \frac{\partial t}{\partial x} \quad (17)$$

An analytical solution of this equation cannot be obtained without many simplifying assumptions, because of its non-linearity. Two new procedures for solving this equation are presented in this section. Another method, similar to one developed by Martinelli, (12), has been used with eddy conductivities predicted by equation (16) to show how this relation may be applied.

Steady State Solution

The last mentioned procedure will be described first. Unlike the others, it has been applied to a wide range of

Reynolds and Prandtl numbers. From the definition of the eddy conductivity, one may write

$$\frac{\dot{Q}}{C_p \sigma} = (\epsilon_c + k) \frac{dt}{dr} \quad (18)$$

Martinelli, (12), has introduced the assumption that $\dot{Q} = \dot{Q}_0 2r/D$. This allows the problem to be treated by means of equation (18), an ordinary differential equation. The more difficult solution of (17), a non-linear partial differential equation is avoided.

It should be noted that the dimension x , in the direction of flow, is eliminated from the problem in this fashion. If the answer desired is a temperature distribution, it will be obtained in the form of $\frac{t_w - t}{t_w - t_{av}}$ as a function of radial position only, for given conditions. If a prediction of total heat transfer is wanted, the result will be the Nusselt number as a function of the Reynolds and Prandtl numbers. The Nusselt number is defined by

$$\text{Nusselt number} = Nu = \frac{\dot{Q}_0 D}{k(t_w - t_{av})} \quad (19)$$

It is found, experimentally, (15), and theoretically, later in this paper, that Nu is unusually high at small values of x/D . Martinelli's assumption precludes detection of this effect.

Equation (18) now takes the form

$$\frac{\dot{Q}_0}{c_p \sigma} \left(\frac{2r}{D} \right) = (\epsilon_c + K) \frac{dt}{dr} \quad (20)$$

This result may now be rearranged into dimensionless form to give

$$\frac{\dot{Q}_0 D}{k(t_w - t_{AV})} \left(\frac{k}{c_p \mu} \right) \left(\frac{2r}{D} \right) = \frac{\epsilon_c + K}{\nu} \frac{d \left(\frac{t_w - t}{t_w - t_{AV}} \right)}{d \left(\frac{r}{D} \right)} \quad (21)$$

Recalling the definitions of Nusselt and Prandtl numbers, we see that equation (20) may be rewritten as

$$\frac{d \left(\frac{t_w - t}{t_w - t_{AV}} \right)}{d \left(\frac{r}{D} \right)} = \frac{Nu}{Pr} \left(1 - 2 \frac{r}{D} \right) \frac{1}{\frac{\epsilon_c}{\nu} + \frac{1}{Pr}} \quad (22)$$

in terms of y , the distance from the pipe wall. Integrating and averaging both sides of the equation between the pipe wall and centerline, we find

$$\frac{Nu}{Pr} = \frac{1}{\int_0^{1/2} \frac{(1 - 2y/D) d(y/D)}{(\epsilon_c/\nu + 1/Pr)}} \quad (23)$$

or $\frac{Nu}{Pr}$ equals the reciprocal of this averaged integral.

In contrast to Martinelli's procedure, which was entirely analytical, calculations have been made from equation (22) by numerical integration. Values of $\frac{(1 - 2y/D)}{(\frac{\epsilon_c}{\nu} + \frac{1}{Pr})}$

were tabulated at appropriate intervals and integrated by summation to a series of values of y/D . Then a second integration was performed to carry out the averaging. At high Prandtl numbers, where the first integral reaches nearly its maximum value in the immediate vicinity of the wall, this integration has been performed only out to $y^+ = 100$. An analytical method was derived for evaluating the small increment in this integral in the center portion of the stream.

In obtaining ϵ_c/ν , Karman's concept of dividing the stream into a laminar layer, near the wall, a buffer layer, and a turbulent core has been retained. In the laminar layer, ϵ_v and ϵ_c are assumed to be zero. In the buffer layer which has been chosen by Karman, (3), to extend between y^+ of 5 and 30, his equation

$$\frac{\epsilon_{v+2}}{\nu} = \frac{(1 - \frac{2y}{D}) Re \sqrt{5/2}}{5} \quad (24)$$

has been used. In the turbulent core, the relation

$$\frac{\epsilon_{v+2}}{\nu} = \frac{(1 - \frac{y}{D}) Re \sqrt{5/2}}{2.5} \quad (25)$$

has been employed. This equation, for flow between parallel plates*, is shown as the upper curve in Figure 2. A best

* Between parallel plates, the Reynolds number is calculated using twice the plate separation as the hydraulic diameter. A compensating factor of two was introduced into equation (24) in obtaining the curve in Figure 2.

fit line through the points on this plot was not used because part of this work was done before these experimental data were available. After values of ϵ_v/ν were obtained at necessary points, ϵ_c/ϵ_v was read from a large scale plot of Figure 4, and ϵ_c/ν calculated accordingly.

The results obtained by this procedure are shown in Figures 5 - 8 together with curves of Karman and Martinelli. The treatment of Karman is quite similar to that of Martinelli, except that the thermal conductivity of the fluid is neglected in the turbulent core. Inspection shows that these authors' results differ only at low Prandtl numbers. Here the laminar and buffer layer resistances have become small due to the high conductivity of the fluid.

The equation obtained by Karman, (3), is

$$S_T = \frac{f/2}{1 + 5\sqrt{f/2} \left\{ (Pr-1) + \ln \left[1 + \frac{5}{6}(Pr-1) \right] \right\}}$$

in the present nomenclature. Martinelli's relationship, (12), has the somewhat different form

$$S_T = \frac{\alpha \sqrt{f/2} \left(\frac{t_w - t_c}{t_w - t_{av}} \right)}{5 \left[\alpha Pr + \ln(1 + 5\alpha Pr) + 0.5 F \ln \left(\frac{Re}{60} \sqrt{f/2} \right) \right]}$$

Martinelli presents curves for the ratio $\frac{t_w - t}{t_w - t_{av}}$ and for

the factor F . This factor is essentially unity for values of the Prandtl modulus above 1.0.

At a Reynolds number of 200,000 the predictions are compared with experimental data on heat transfer to gases, and mercury, in Figures 5 and 6. The present work is seen to agree most satisfactorily with the experimental data on mercury. It differs from Martinelli's work only in using values of ϵ_c/ϵ_v from 0.1 - 0.4 instead of unity. Since gases have $Pr = 0.74-0.85$, Figure 4 predicts $\epsilon_c/\epsilon_v = \text{unity}$ throughout nearly the entire fluid, and the present analysis becomes identical with that of Martinelli.

Figures 7 and 8, for a Reynolds number of 10,000 present a rather different picture. Here, the region of the curves at values of Pr above 1.0 have received greatest experimental attention. The theoretical curves give reasonable approximations to the data points up to Prandtl number of 50. Here the data become much more uncertain, but Reichardt's prediction seems too high, with the writer's and Martinelli's lines being too low.

It may be noted, in Figure 7, that all the predictions approach constant, limiting values of the Nusselt number as asymptotes. At these high values of the Prandtl number, all the heat transfer theories give the result

$$Nu = \frac{Re \sqrt{f/2}}{\gamma_1^+} \quad (26)$$

where y_1^+ is the value of y^+ assigned to the inner boundary of the laminar sublayer. This value is approached because all of the other resistances to heat transfer become negligible in this region.

In the light of equation (26), the fact that Reichardt used a value of $y_1^+ = 2$ clearly explains the difference between his curve and those of the author and Martinelli, which were both based on $y_1^+ = 5$. It is noteworthy that whereas the writer's line is quite close to that of Martinelli for $Pr > 1$, Reichardt's values become very different. The fact that in the present work, at $Pr = 100$, values of ϵ_c/ϵ_v from 2 to 5 instead of unity, affected the result hardly at all.

In contrast, the quite small change introduced in Reichardt's velocity distribution near the wall has caused a very large change in the predicted Nusselt number. In Figure 9, a comparison of these velocity curves with available experimental data is shown. The scatter in the points is such as to render any choice between the two lines difficult, if not impossible.

Such a skeptical position is further encouraged if one reads of Laufer's experimental difficulties. As then used, the hot-wire technique was found to give unexpectedly high velocities near the channel boundary. This was explained as heat conduction to the wall. Data were then

taken with a lower hot-wire operating temperature, and were found to be of the expected magnitude. These latter values are those used in Figure 9. Since Reichardt's measurements were also obtained with a hot-wire, this difficulty is likely to be present in his data also.

It should be noted that between y^+ of 2 and 5, according to the lower curve, ϵ_v is quite small compared to ν , but at $Pr \approx 100$, ϵ_c is large compared to K , which is only $1/100$ of ν . This illustrates one of the fundamental difficulties of predicting heat transfer at high Prandtl numbers from velocity data. Even if ϵ_c/ϵ_v were known satisfactorily, it is extraordinarily difficult to measure ϵ_v when it is small compared to ν . Experiments on the temperature distribution near such a heated wall will be much more useful, and probably much easier to obtain.

Unsteady State Solutions

Two methods of treating the overall heat transfer problem have been developed which show variations in Nusselt number and temperature profile with longitudinal position. Both of these solve the partial differential equation (17). The first of these procedures uses an analogous electrical circuit. The other technique is an iterative numerical solution which is applied to a finite difference form of equation (17). Many problems in localized or intermittent

heating of fluids are susceptible to solution in this fashion that otherwise would have to be by-passed entirely.

The electrical circuit considered to be analogous to the present physical situation is shown in Figure 10. In this grid, the successive junction points between resistors correspond to successive points along a radius of the tube, and the resistances connecting them represent the lumped thermal resistance of the intervening liquid. The time dimension of the electrical network corresponds to distance in the direction of flow, making the current flow into the condensers analogous to the rate at which thermal energy is removed by transport with the flowing stream. The fluid temperature at a given radius is then represented by the network voltage at the corresponding point, and its variation with distance downstream from the entrance is represented by the variation of this voltage with time elapsed since closing the rotary switch.

The average velocity of the fluid at any point, and the corresponding eddy viscosities have been evaluated by the same procedure used in the steady state treatment. However, since the equations developed in the preceding section, relating ϵ_c and ϵ_v were not available at the time of this work, these quantities were assumed equal. Since calculations by means of this analogy have been performed only for water, the values of ϵ_c/ϵ_v predicted would have

been close to unity, and the results would have been essentially the same.

The analogous electrical circuit shown in Figure 1 may be justified by intuitive physical reasoning or by an analytical derivation.

An approximate representation of equation (17), may be obtained using the finite difference expression that is indicated below.

$$\frac{r_{32}(K+\epsilon_c)_{32}(t_3-t_2) - r_{21}(K+\epsilon_c)_{21}(t_2-t_1)}{(\Delta r)^2} = r_2 u_2 \left(\frac{dt}{dr} \right)_2 \quad (27)$$

In this equation, the subscripts refer to a series of points at various radial distances for given longitudinal positions in the stream.

In the analogous electrical circuit, the response is governed by the relationship

$$\frac{V_3 - V_2}{S_{32}} - \frac{V_2 - V_1}{S_{21}} = C_2 \left(\frac{dV}{d\theta} \right)_2 \quad (28)$$

In equation (28), S denotes electrical resistance and θ represents time. Inspection of equations (27) and (28) yields the following analogies:

Temperature	\sim	voltage
$ru \Delta r$	\sim	capacitance
$\Delta r/r(K+\epsilon_c)$	\sim	electrical resistance

downstream ~ time
distance

Such an analogy has been utilized on the analog computer of this institute, (16), to find temperature distribution in a turbulent stream. In order that results could be compared with experimental data, operating conditions were chosen which corresponded to the conditions reported by Sherwood and Petrie, (17). These operating variables and results in each case are presented in Table I. The calculated values of thermal flux and temperature difference between the fluid and the wall were combined to yield an effective thermal transfer coefficient. The average temperature was determined by integration of the product of the temperature and the point velocity, divided by the average velocity. The procedure established the temperature of the mixed fluid after equilibrium had been reached at a particular section. The curve obtained in this fashion for case B is shown in Figure 11.

The voltage measurements were made with a cathode-ray oscilloscope which recorded the electromotive force as a function of time. A typical photographic record is shown in Figure 12. The curves were smoothed graphically with respect to the analogs of temperature and radial distance. Figures 13 and 14 correspond to case A of Table I and Figures 15 and 16 relate to case B.

The change in voltage across the first resistor of the network provided a means of determining the thermal flux at any point. This resistor was considered to represent a point within the laminar sublayer. Consequently the thermal flux was equal to the product of the thermal conductivity and the radial temperature gradient. This was determined from the voltage drop across the first resistor.

The results of these calculations are shown in Table I. They are in reasonable agreement with the experimental data but some significant differences exist. It is probable that these differences may be ascribed to the following sources of error:

- (1) Uncertainty in the values of ϵ_c as predicted from both isothermal and non-isothermal flow.
- (2) The distortion of streamlines by natural convection as a result of temperature gradients.
- (3) The use of finite difference approximations in the solution of the differential equation.
- (4) Deviations in the resistances and capacitances used from values stipulated by the analogy, and the limited precision resulting from the relatively small size of oscilloscope used.

In this instance, the uncertainty in ϵ_c is the predominant source of error. Reference to Figure 2 shows the minimum deviation which may be expected in ϵ_c since

speculation as to ϵ_c/ϵ_v is also present.

The equipment used for electrical analogy measurements only permits the circuit parameters to be established within about 5 per cent in some cases. This was a result of the wide variation in relative values of resistance and capacitance that was needed in the solution of this problem. By the use of larger circuit elements and a correspondingly longer time for each measurement the uncertainty may be decreased.

However, it seems likely that for most purposes, the iterative numerical solution of equation (17) will be found more appropriate. In this case, the differential equation has been replaced by the finite difference expression

$$\frac{r_{32}(K+\epsilon_c)_{32}(t_3-t_2) - r_{21}(K+\epsilon_c)_{21}(t_2-t_1)}{(\Delta r)^2} = r_{2-u_2} \frac{(t_u - t_2)}{\Delta x} \quad (29)$$

where t_u is the temperature at the same radius as point 2, but one interval downstream. For convenience, this expression has been rewritten in the dimensionless form

$$\frac{\left(\frac{r_{23}}{D}\right)\left(\frac{K+\epsilon_c}{\nu}\right)_{23}\left(\frac{t_3-t_2}{t_w-t_0}\right) - \left(\frac{r_{21}}{D}\right)\left(\frac{K+\epsilon_c}{\nu}\right)_{21}\left(\frac{t_2-t_1}{t_w-t_0}\right)}{\Delta\left(\frac{r}{D}\right)^2} \quad (30)$$

$$= \frac{\left(\frac{r_2}{D}\right)\left(\frac{Du}{\nu}\right)\left(\frac{t_4-t_2}{t_w-t_0}\right)}{\left(\frac{\Delta x}{D}\right)}$$

Equation (30) has been further abbreviated for computational use into the form

$$\overline{T}_A - \overline{T}_2 = \overline{\Phi}_{2,2} (\overline{T}_3 - \overline{T}_2) - \overline{\Phi}_{1,2} (\overline{T}_2 - \overline{T}_1) \quad (31)$$

where

$$\overline{\Phi}_{1,2} = \frac{\left(\frac{K + \epsilon_c}{\nu}\right)_{z_1} \left(\frac{\Delta x}{D}\right) \left(\frac{\tau}{D}\right)_{z_1}}{\left(\frac{D u}{\nu}\right)_1 \left(\frac{\Delta \tau}{D}\right)^2 \left(\frac{\tau}{D}\right)_2} \quad (32)$$

From these definitions, T has a value of 0.0 at the boundary $x = 0$, and a value of 1.0 at the boundary $r/D = \frac{1}{2}$. Consequently, the entire temperature field in the problem is obtained by successive application of equation (31), beginning at the upstream boundary and proceeding in the direction of flow.

This procedure has been applied to the heating of liquid mercury, at a Reynold's number of 200,000, and a Prandtl number of 0.0056. The interval, $\frac{\Delta \tau}{D}$, was chosen as 0.1, with points taken equally spaced between the wall and the centerline. S. Frankel has recently prepared a paper, (18), in which it is shown that, for the case where ϕ is constant, its value must be equal to or less than one-half, if the solution is to be convergent. On this basis, the interval, $\frac{\Delta x}{D}$, was chosen as 2.0; this gave a value of ϕ on

one side of a point which was 0.59, but the value on the opposite side was 0.21. Quite satisfactory convergence was obtained. The format used in this case, with sample calculations shown, is given in Appendix II.

A plot of the Nusselt number as a function of longitudinal position for this case is shown in Figure 17, together with the value calculated by the steady-state procedure. The agreement is considered quite satisfactory, particularly in view of the difference in the assumptions made in the two solutions. It is noted that the value of the Nusselt modulus obtained for x/D of 10 is less than 7% higher than the asymptotic value. This is in marked contrast to the result of Sanders, (19), who predicts them even at 100 diameters, the Nusselt number is more than 20% above its asymptotic value. His unsteady-state treatment is based only on consideration of the region very near the wall. Since this region is of minor importance at low Prandtl numbers, his unreasonable result is not surprising.

A chart has been prepared to summarize the qualitative conclusions which have been drawn about the influence of the Prandtl number on the various factors governing overall heat transfer inside tubes. This chart is presented in Figure 18. It is hoped that it will give the reader a better picture of the application of the developments given in this paper, and of the need for future experimental work.

MOMENTUM AND THERMAL TRANSFER IN
NON-UNIFORM TURBULENT FLOW

The present status of experimental and theoretical work on the relationship between heat transfer and friction in non-uniform turbulent flow does not permit precise evaluation of ϵ_c/ϵ_v under any conditions. The work of several investigators, (20), (21), (10), indicates that this ratio lies between 1.0 and 2.0, but the variations are such that no more definite conclusion may be drawn.

The principal theoretical developments in this field are ^{the} momentum transfer hypothesis of Prandtl, (4), and the vorticity transfer theory of Taylor, (5). Prandtl's work has been briefly summarized here in the discussion of the effect of fluid properties on ϵ_c/ϵ_v . Even prior to this, Taylor pointed out, (22), that as an eddy moved between two layers in the fluid, its momentum might be changed by pressure gradients in the fluid, contrary to Prandtl's assumption.

Taylor proposed, as an alternative, that, in two dimensional flow, the vorticity of an eddy be assumed invariant in its motion through the fluid. Under these conditions, the vorticity may be written as $\frac{1}{2} (\partial u/\partial y)$. The concentration gradient of vorticity is then $\frac{1}{2} (\partial^2 u/\partial y^2)$. The rate of vorticity transfer has been shown, (5), to be equal to $2\rho (\partial \tau/\partial y)$. Since the concept of eddies being

created, traveling a distance equal to the mixing length, and then being destroyed is retained, lv' is still a "diffusion coefficient" for the eddies. Consequently, we may combine the above quantities to yield

$$\partial \tau / \partial y = \rho lv' \left(\frac{\partial^2 u}{\partial y^2} \right) \quad (33)$$

Unless the nature of the variation of lv' is known, (33) does not yield a direct solution.

If it should be assumed that over a region, lv' is constant, the above relation may be integrated to give

$$\tau = \frac{1}{2} \rho lv' \left(\frac{du}{dy} \right) \quad (34)$$

Comparison of equations (1), (11), and (34) shows that we now have the relation $\epsilon_c = 2\epsilon_v$. The recent experimental data obtained in this department, shown in Figure 1, have demonstrated that this relation is not valid in uniform flow. In fact, the rival theory of Prandtl has been verified for this case.

However, the recent measurements of Mason, (10), in the wake of a heated cylinder have demonstrated that values of ϵ_c/ϵ_v considerably higher than unity can be obtained under such conditions. Corrsin and Uberoi, (21), have made direct measurements of Q , τ , dt/dy in heated air jets, and have found ϵ_c/ϵ_v to lie between 1.3 and 1.4. Page and

Falkner, (23), have presented experimental evidence in support of Taylor's hypothesis, although direct calculations of ϵ_c and ϵ_v were not made.

Prandtl has suggested a possible physical basis for a difference in the nature of channel flow and the non-uniform flow of wakes and jets, (24). Near the trailing edge of an obstacle in an open stream, fluid is being transformed from its undisturbed approach into highly turbulent motion. The orientation of the fluctuating velocity components is probably closely determined by the position of the obstacle. For example, if the flow approaches a cylinder perpendicular to its axis, the turbulent motion will be two-dimensional, with fluctuations in the direction of the cylinder axis being practically negligible. As opposed to this picture, fully developed turbulence in a channel has had ample time for equilibrium to be established between the various components of the fluctuation. It has long been known that in this equilibrium condition, the turbulence attains a high degree of isotropy. In fact, Fage and Townend, (25), have shown that near a wall, the most violent fluctuations are perpendicular to the plane of flow.

Since Taylor's theory is derived on the premise that the disturbances are two-dimensional, it should not be surprising if his predictions were to be at least approximately fulfilled in the wake of obstacles, and in jets, where this

condition is met.

An empirical study of the temperature and velocity curves in heated jets has been made. The data of several workers have been compared by plotting $\frac{t-t_s}{t_0-t_s}$ as a function of $\frac{u}{u_0}$. The resulting graph is shown in Figure 19. Under assumptions generally made in integrating the basic partial differential equation, (5), the slope of the line in this plot represents the local value of ϵ_c/ϵ_v . Thus the data is seen to correspond more closely to $\epsilon_c = 2\epsilon_v$ far downstream in the jet, rather than near the mouth, as would be expected on the basis of Prandtl's reasoning.

Regardless of whether the various turbulence theories are in agreement with the points, the plot in Figure 19 is considered by the author to give a valuable correlation. In this fashion, the temperature distribution to be expected in a jet can be predicted directly from a knowledge of the velocity distribution. When this latter information is not known experimentally, it may be predicted by several procedures now available.

It should be emphasized that in non-uniform turbulent flow, temperature fields are governed by the differential equation*

$$\frac{\partial \left[r(K+\epsilon_c) \frac{\partial t}{\partial x} \right]}{\partial r} + r \frac{\partial \left[(K+\epsilon_c) \frac{\partial t}{\partial x} \right]}{\partial x} = ru \frac{\partial t}{\partial x} \quad (35)$$

* The absence of heat sources and sinks within the fluid is assumed here.

This relation is derived in Appendix I. This equation considers turbulent transfer perpendicular to the stream, and also in the direction of the flow. Previous writers, (20), (12), (13), have neglected the eddy conductivity in the direction of flow, simplifying equation (35) to the form

$$\frac{\partial [r(K+\epsilon_c)r \frac{\partial t}{\partial r}]}{\partial r} = ru \frac{\partial t}{\partial x} \quad (36)$$

It follows by integration of this expression that

$$\int_{-\infty}^{\infty} ru t dr = \text{constant} \quad (37)$$

This integral is proportional to the rate of enthalpy flow in the direction of the stream.

The data of Corrsin, (26), on flow in heated jets has been used to calculate values of the above integral. The ratio of these values to the integral at the jet mouth has been plotted distance downstream in Figure 20. According to equation (37), a constant ratio of unity should be obtained. Unexpectedly, the curve drops as low as 60%. Returning to equation (35), it is seen that this decrease must be due to turbulent transfer along the jet axis.

REFERENCES

1. O. Reynolds, Proc. Manchester Lit. and Phil. Soc., 14, 7, (1874).
2. L. Prandtl, Phys. Zeit., 29, 487, (1928).
3. Th. von Karman, Trans. A.S.M.E., 61, 705, (1939).
4. L. Prandtl, Phys. Zeit., 11, 1072, (1910).
5. G. I. Taylor, Proc. Roy. Soc. (London), A135, 685, (1939).
6. J. Nikuradse, Forschungsheft, VDI, 361, 1, (1933).
7. T. K. Sherwood and B. B. Woertz, Ind. Eng. Chem., 31, 457, (1939).
8. W. L. Towle and T. K. Sherwood, Ind. Eng. Chem., 31, 1034, (1939).
9. W. G. Schlinger, and B. H. Sage, to be published in Chem. Eng. Progress.
10. D. M. Mason, Ph.D. thesis, Calif. Inst. of Tech., June 1949.
11. L. M. K. Boelter, R. C. Martinelli, and F. Jonassen, Trans. A.S.M.E., 63, 447, (1941).
12. R. C. Martinelli, "Further Remarks on the Analogy Between Heat and Momentum Transfer", Paper presented at Sixth International Congress for Applied Mechanics; Paris, France; Sept. 1946.
13. H. Reichardt, Zeit. fur Ang. Math. & Mech. 20, 297, (1940), also N.A.C.A. T.M. 1047.
14. H. S. Carslaw and J. C. Jaeger, "The Conduction of Heat in Solids", p. 202 3rd edition, Cambridge Univ. Press., 1948.
15. A. Cholette, Chem. Eng. Prog., 44, 81, (1948).
16. G. D. McCann, C. H. Wilts, and B. Locanthi, "Electronic Technique Applied to Analog Methods of Computation", Trans. Inst. Radio Engrs., (to be published).

17. T. K. Sherwood, and J. M. Petrie, *Ind. Eng. Chem.*, 24, 736, (1932).
18. S. Frankel, "The Rate of Convergence of Relaxation Method Calculations", California Institute of Technology, 1949.
19. V. D. Sanders, "A Mathematical Analysis of the Turbulent Heat Transfer in a Pipe with a Surface Temperature Discontinuity at Entrance", M. S. Thesis, University of California, Berkeley, Calif., November, 1946.
20. G. I. Taylor, *Proc. Roy. Soc., (London) Series A*, 215, 1, (1915).
21. S. Corrsin and M. Uberoi, N. A. C. A. Tech. Note 1865, May 1949.
22. G. I. Taylor, *Proc. Roy. Soc., (London)*, A151, 494, (1935).
23. A. Fage and T. P. Falkner, *Proc. Roy. Soc., (London)*, A135, 702, (1932).
24. L. Prandtl, in W. L. Durand's "Aerodynamic Theory", Vol. III, p. 176 & 177, Berlin, Julius Springer, (1935).
25. A. Fage and H. C. H. Townend, *Proc. Roy. Soc., (London)*, A135, 657, (1932).
26. S. Corrsin, N. A. C. A. Wartime Report W-94.
27. W. H. Corcoran, Ph.D. Thesis, Calif. Inst. of Tech., June, 1948.
28. V. Cleaves and L. M. K. Boelter, *Chem. Eng. Prog.*, 43, 123, (1947).
29. P. Ruden, *Naturwissenschaften*, 21, 375 (1933).
30. J. Laufer, Ph.D. Thesis, Calif. Inst. of Tech., June, 1948.
31. F. H. Morris and W. G. Whitman, *Ind. Eng. Chem.*, 20, 234 (1928).
32. A. Eagle and R. M. Ferguson, *Proc. Roy. Soc., (London)*, A127, 540 (1930).
33. M. A. Styrikovitch and I. E. Semenovker, *Jour. Tech. Phys., (U.S.S.R.)*, 10, 1324 (1940).
34. A. P. Colburn and C. A. Coughlan, *Trans. A. S. M. E.*, 63, 561 (1941).

NOMENCLATURE

c	Concentration, lbs/ft ³
c _p	Specific heat at constant pressure, Btu/lb °F
d	diameter, ft.
D	Diffusion coefficient, ft ² /sec.
f	Fanning friction factor, dimensionless
g	Gravitational constant, ft/sec ²
h	Heat transfer coefficient, Btu/hr ft ² °F
H	Enthalpy, Btu/lb
k	Thermal conductivity, Btu/hr ft ² °F
K	Thermal diffusivity, ft ² /sec
l	Mixing length, ft
Q	Rate of heat flow, per unit area Btu/hr ft ²
Q _o	Rate of heat flow per unit area at wall, Btu/hr ft ²
r	Radial distance, ft.
s	Electrical resistance, ohms
t	Temperature, °F
u	Point velocity, ft/sec
u ⁺	$u/\sqrt{\tau_w/\rho}$
V	Average velocity, ft/sec
v	Voltage
x, y, z	Coordinates, ft.
y	Distance from wall, ft.
y _o	Plate separation in two-dimensional flow, or tube diameter, ft.

NOMENCLATURE (Cont'd)

y^+	$\frac{y\sqrt{\tau_0/\rho}}{\nu}$
α	Ratio $\frac{\epsilon_c}{\epsilon_v}$
σ	Density, lbs/ft ³
μ	Viscosity, lbs/sec ft
ϵ_c	Eddy conductivity, ft ² /sec
ϵ_D	Eddy diffusivity, ft ² /sec
ϵ_v	Eddy viscosity, ft ² /sec
ν	Kinematic viscosity, ft ² /sec
ρ	Mass density, lbs sec ² /ft ⁴
τ_0	Shear force at wall, lbs/ft ²
τ	Local shear force, lbs/ft ²
Φ	See equation (32)
\ominus	Dimensionless Groups
Nu	Nusselt number, defined in equation (19)
Pr	Prandtl number, $\frac{c_p \mu}{k}$
Re	Reynolds number, $\frac{DV}{\nu}$
St	Stanton number, equal to $\frac{\text{Nusselt no.}}{(\text{Reynolds no.})(\text{Prandtl no.})}$

Table I

Comparison of Experimental and Calculated Conditions

	Case A	Case B
Reynold's Number	50,800	82,300
Prandtl Number	1.891	1.826
Inlet Water Temperature °F	181.8	184.5
Average Temperature of Tube Wall °F	203.7	203.1
Measured Outlet Temperature °F	192.0	192.3
Calculated Outlet Temperature °F	193.2	194.6

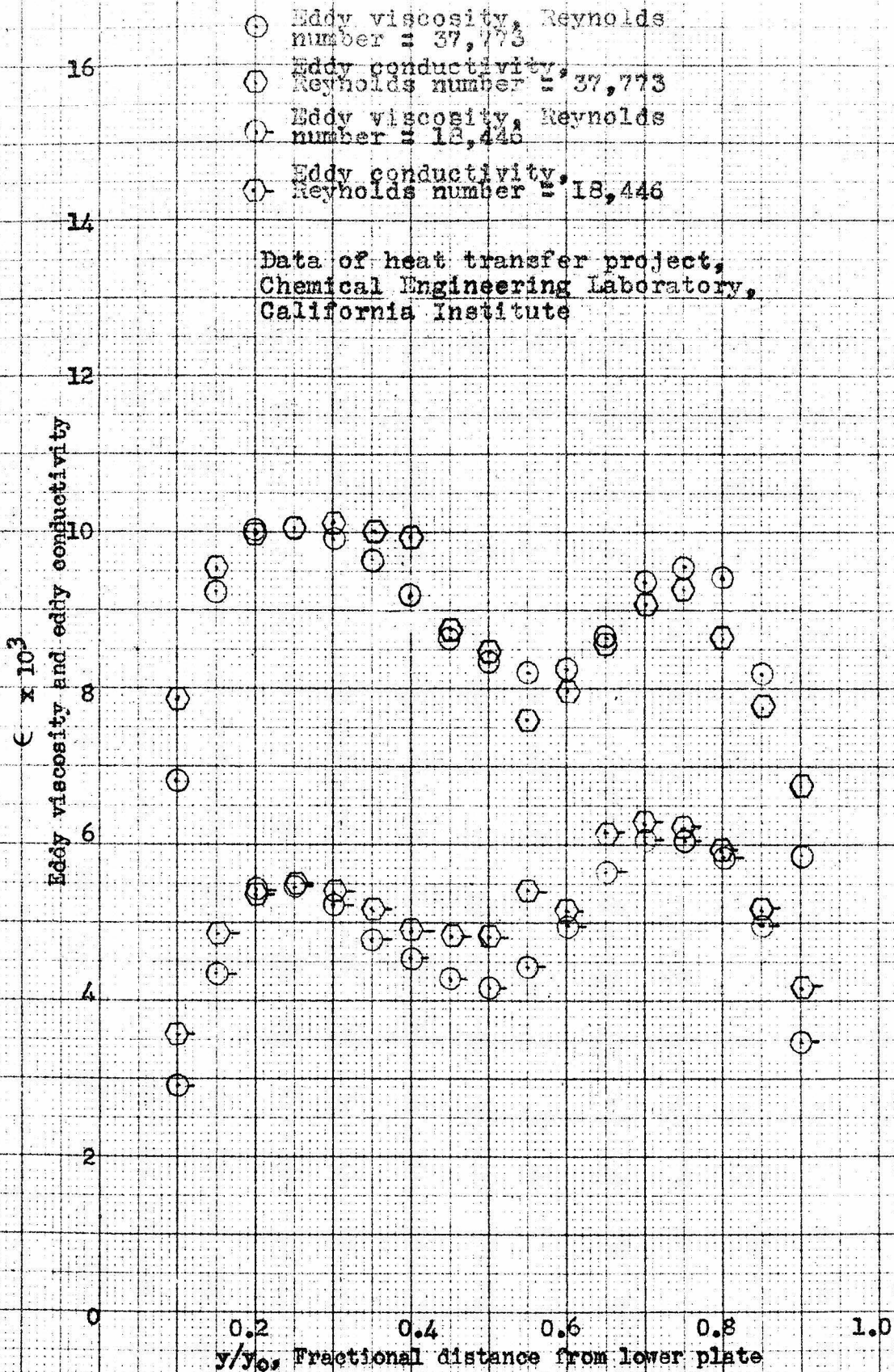


Figure 1. Eddy viscosity and eddy conductivity.

- Eddy viscosity, Reynolds number = 37,773
- Eddy conductivity, Reynolds number = 37,773
- Eddy viscosity, Reynolds number = 18,446
- Eddy conductivity, Reynolds number = 18,446

Data of heat transfer project,
Chemical Engineering Laboratory,
California Institute

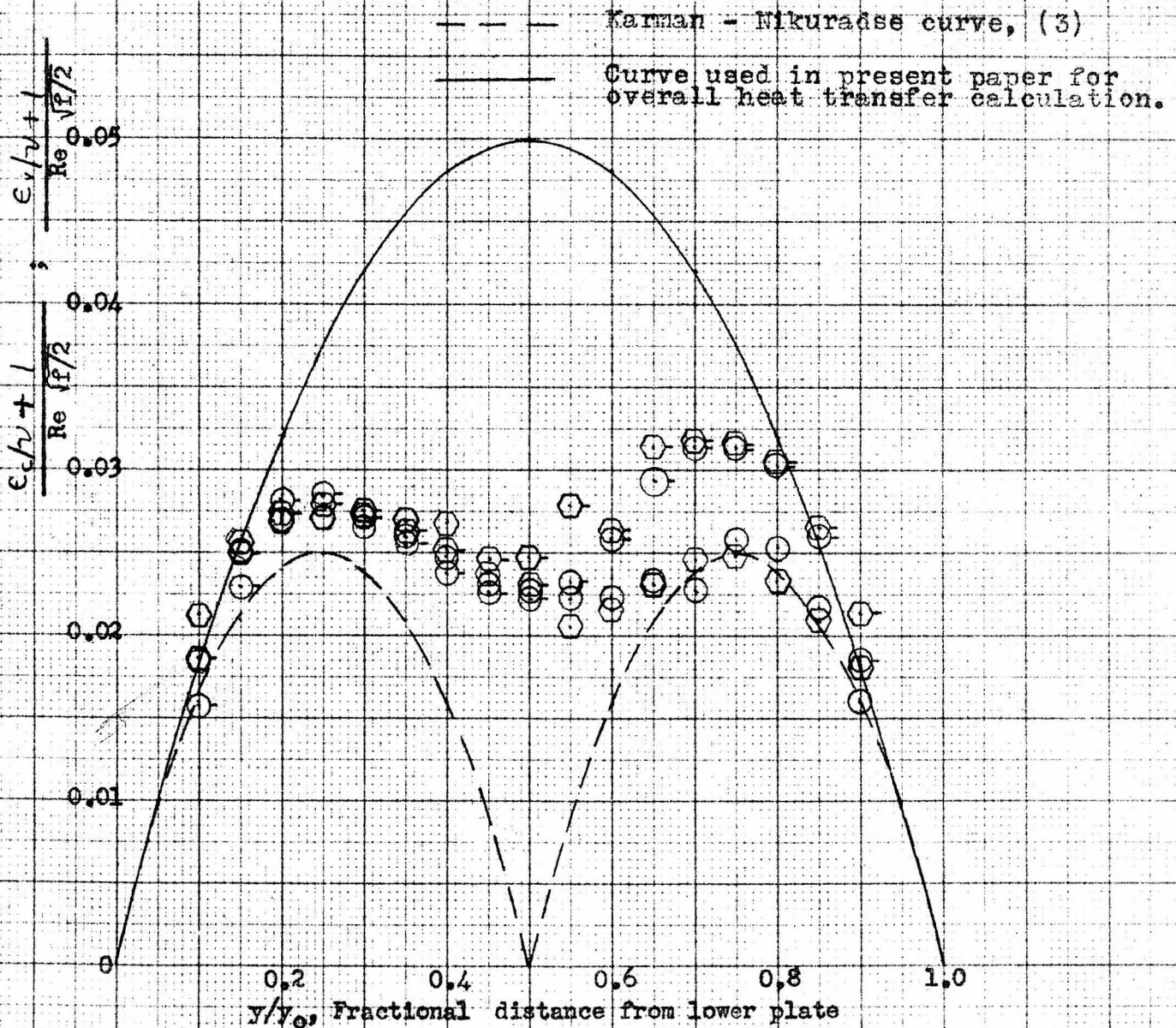


Figure 2. Generalized plot of eddy viscosity and eddy conductivity

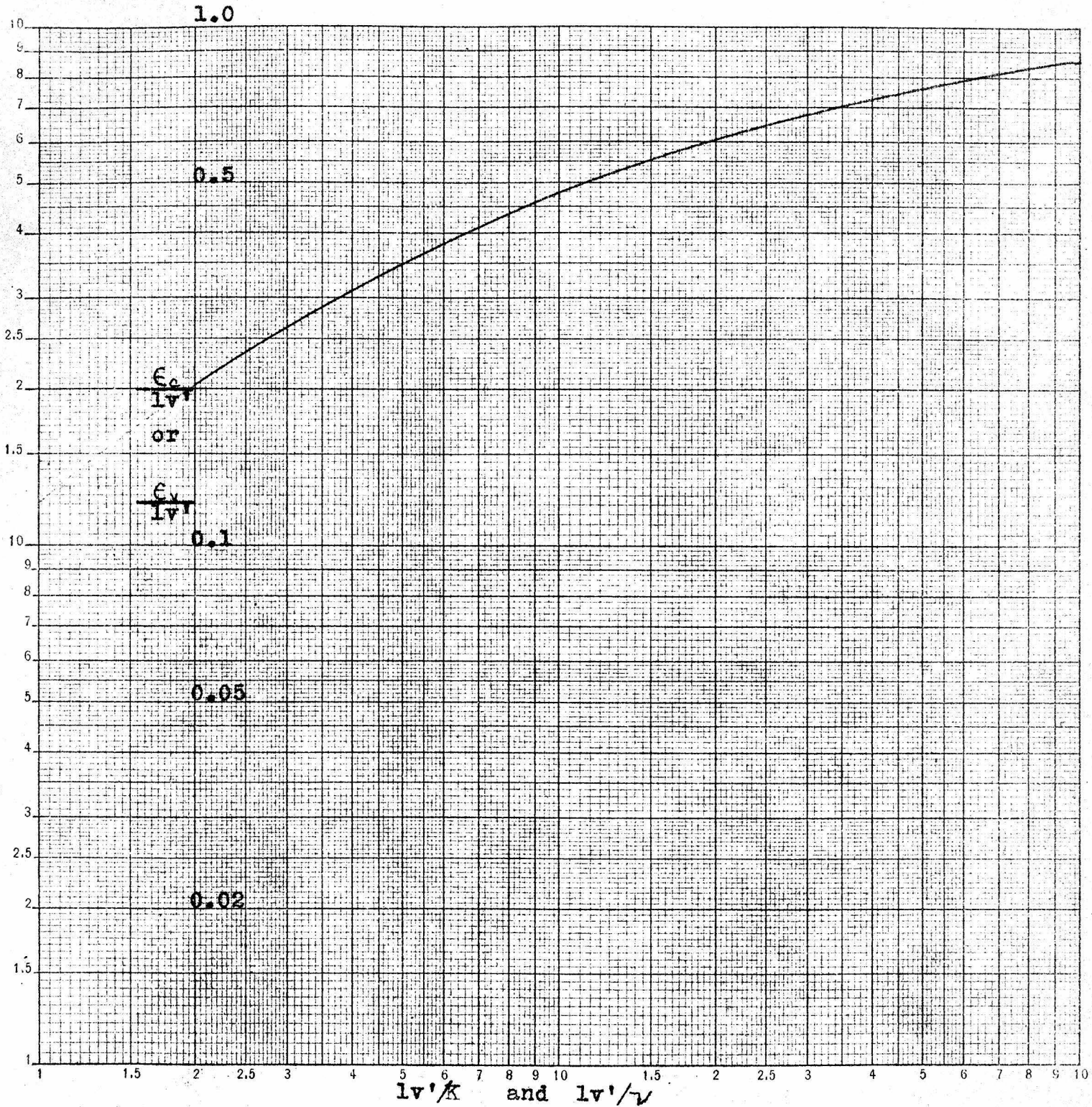


Figure 3. Ratio of eddy conductivity or eddy viscosity to lv' versus lv'/K and lv'/v

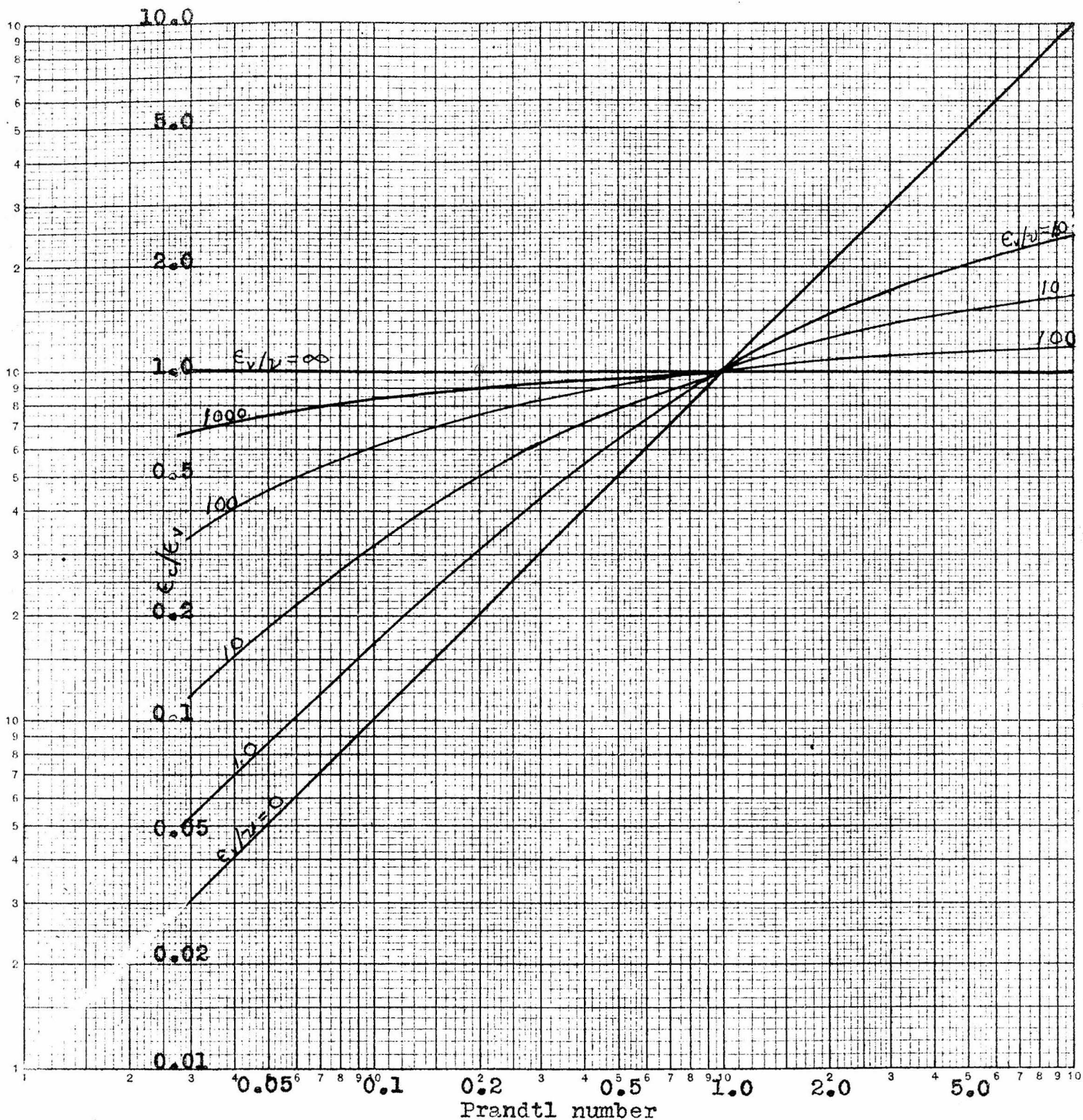


Figure 4. Ratio of eddy viscosity to eddy conductivity as function of Prandtl number

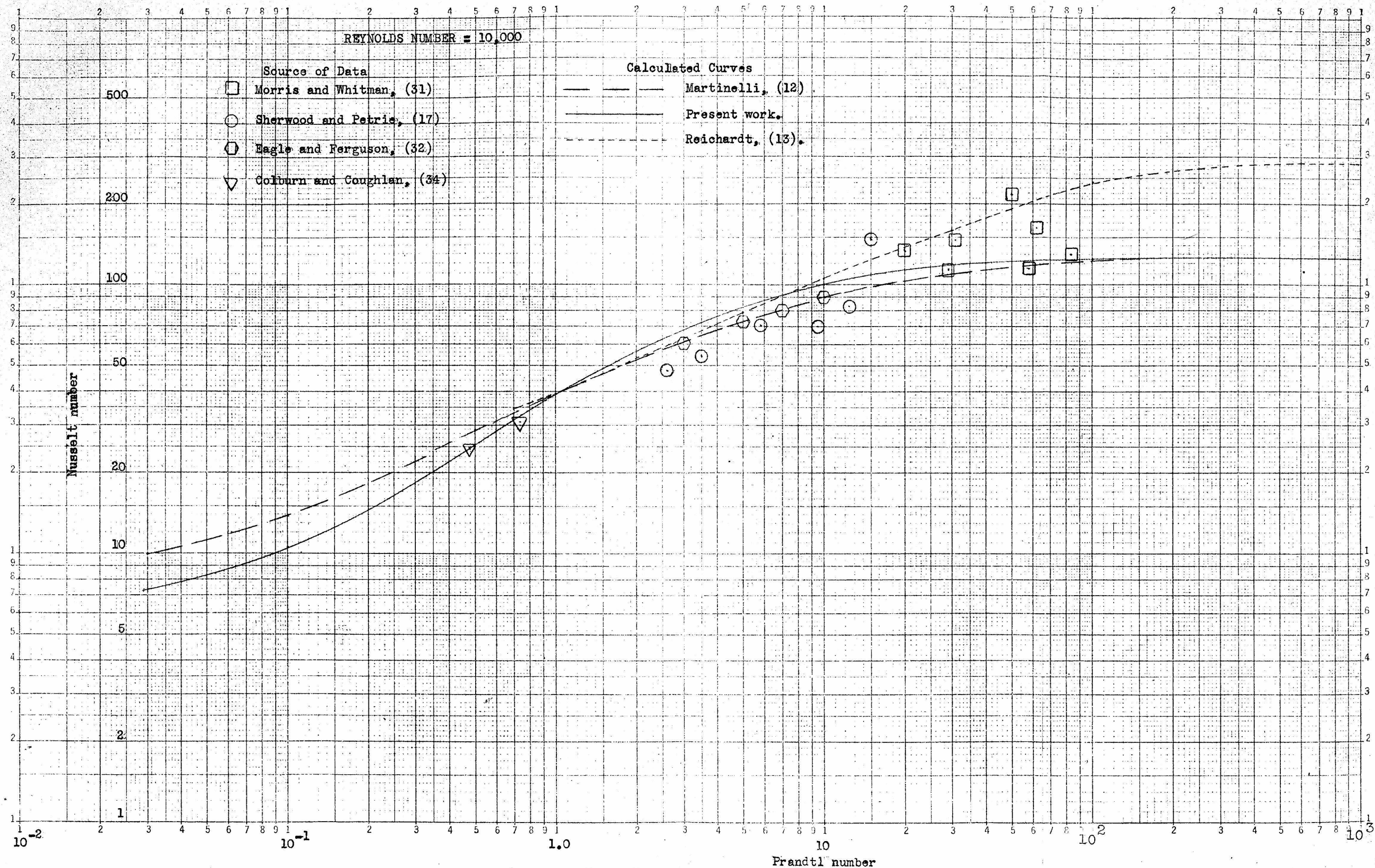


Figure 7 Nusselt number versus Prandtl number

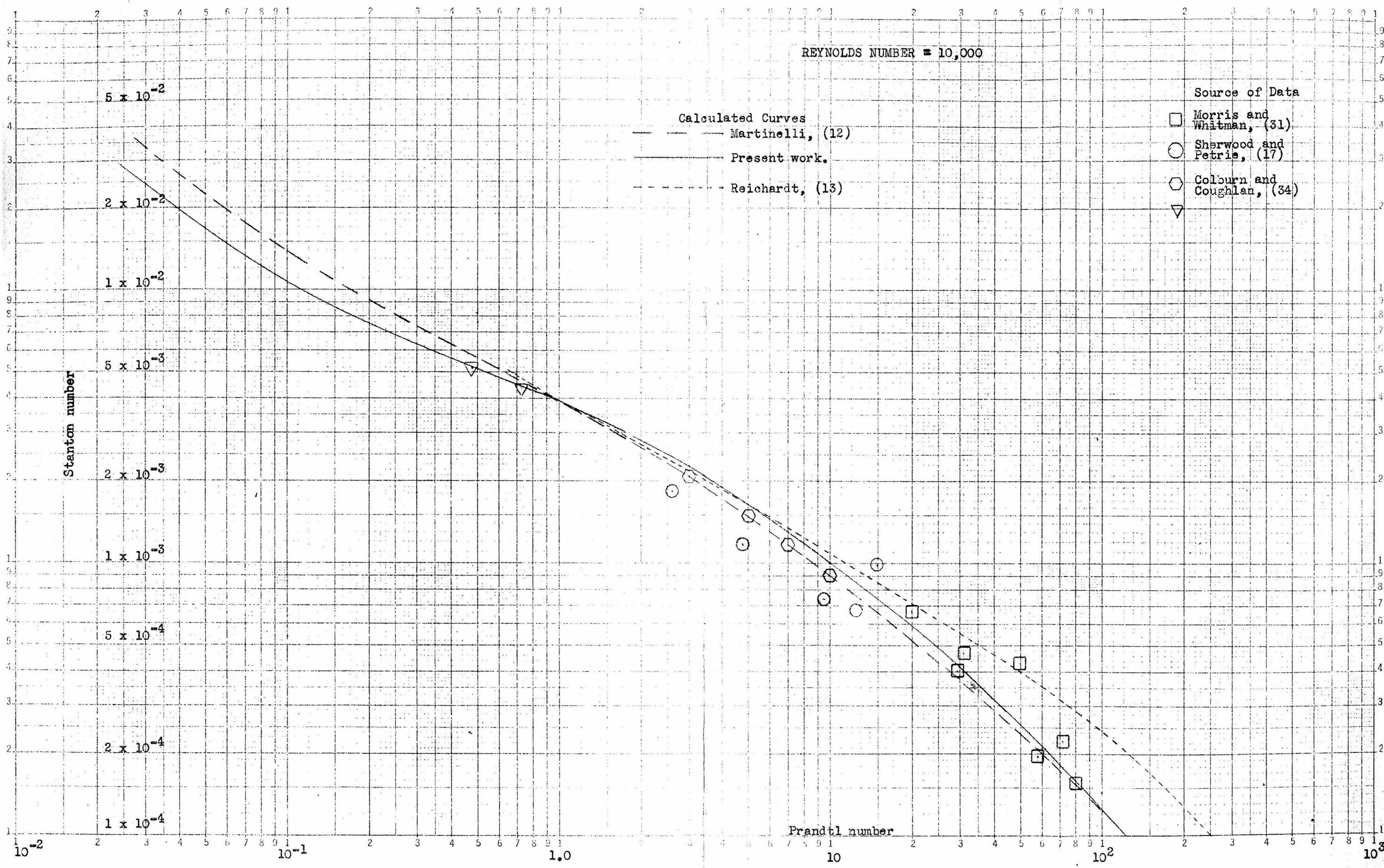


Figure 8. Stanton number versus Prandtl number

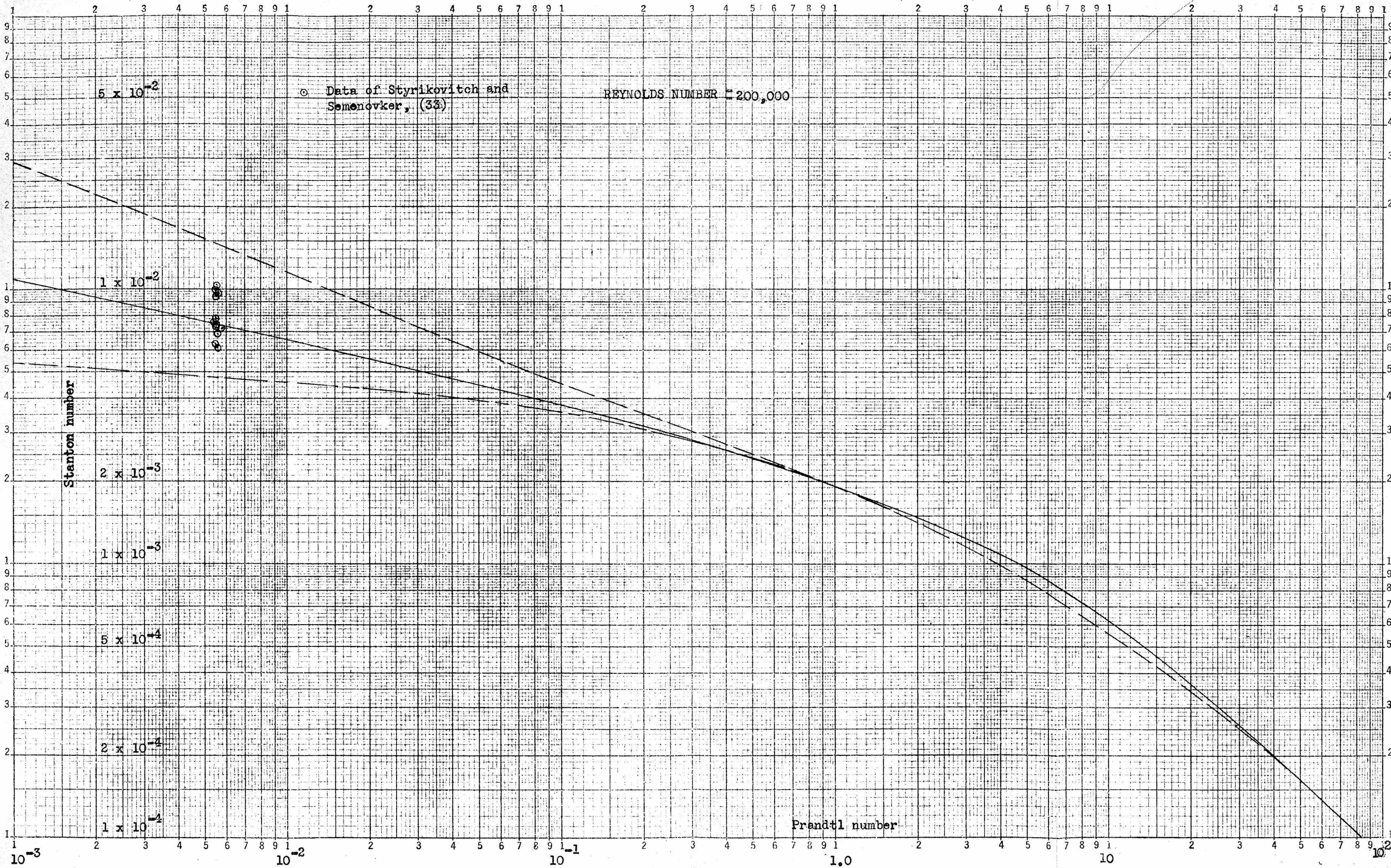


Figure 5. Stanton number versus Prandtl number

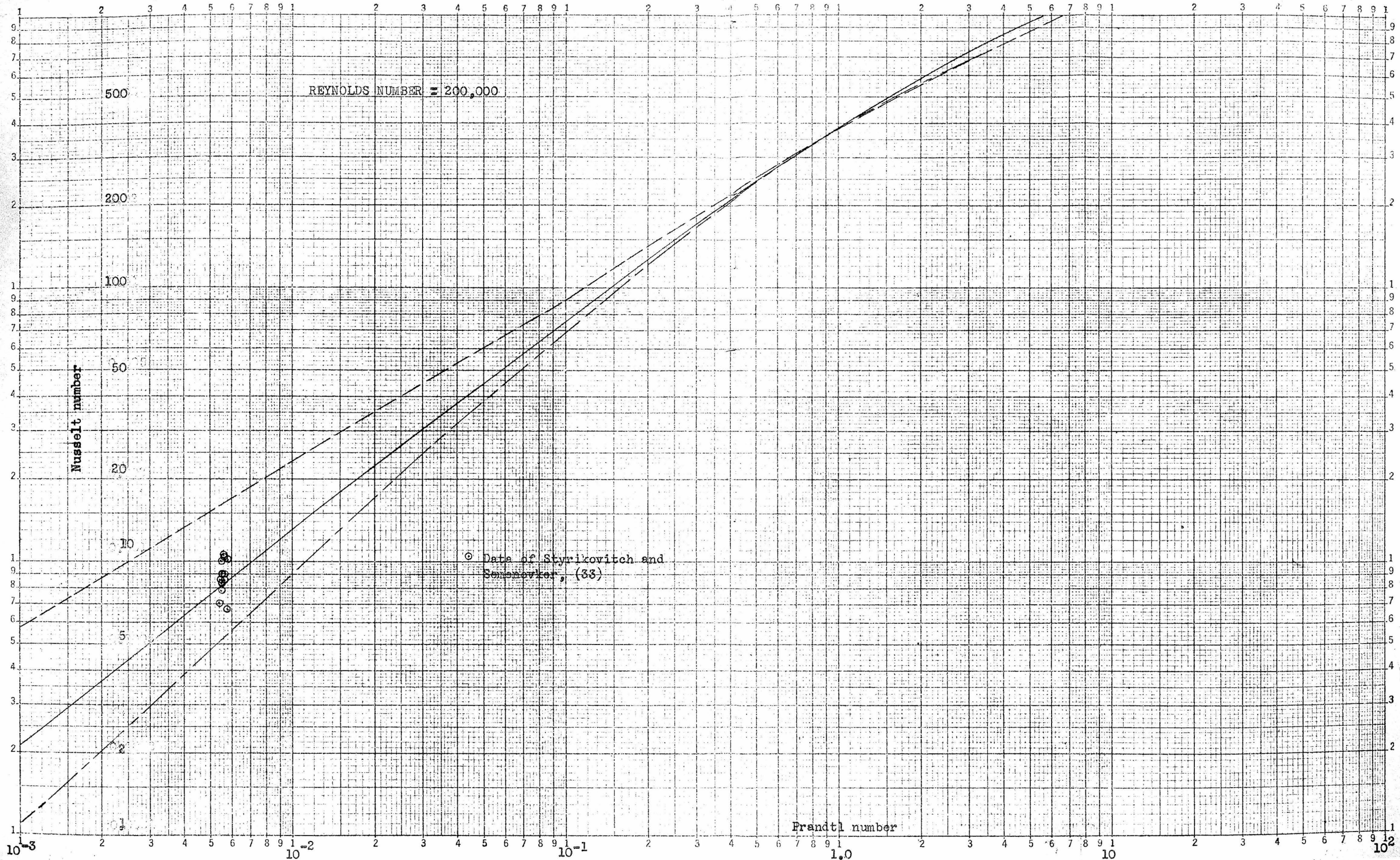


Figure 6. Nusselt number versus Prandtl number

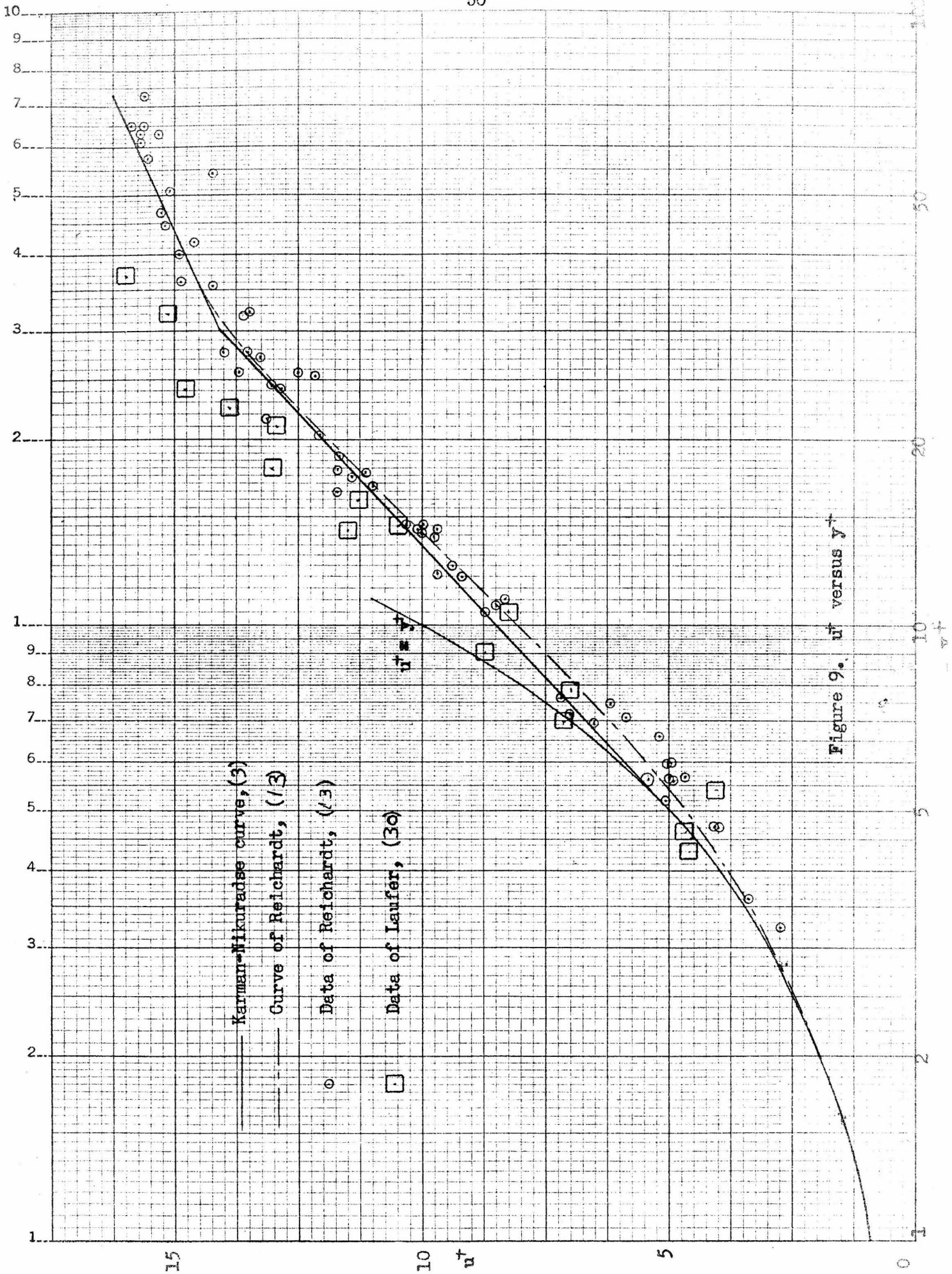


Figure 9. u^+ versus y^+

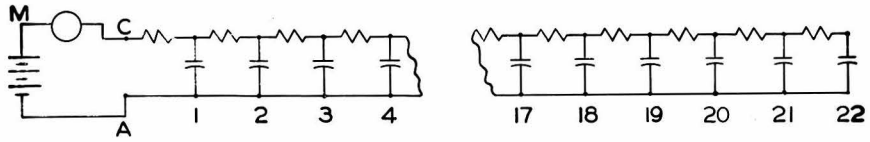


Figure 10. Electrical analogy circuit.

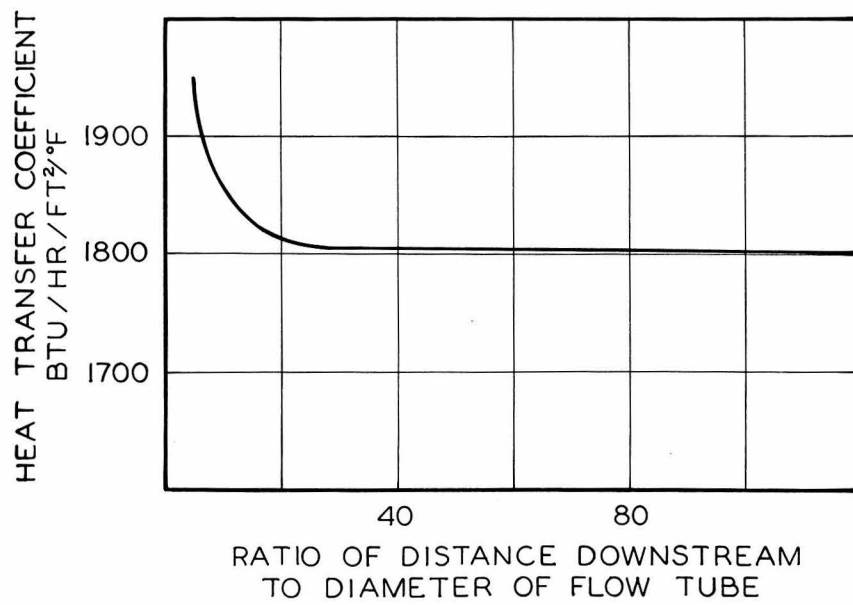


Figure 11.

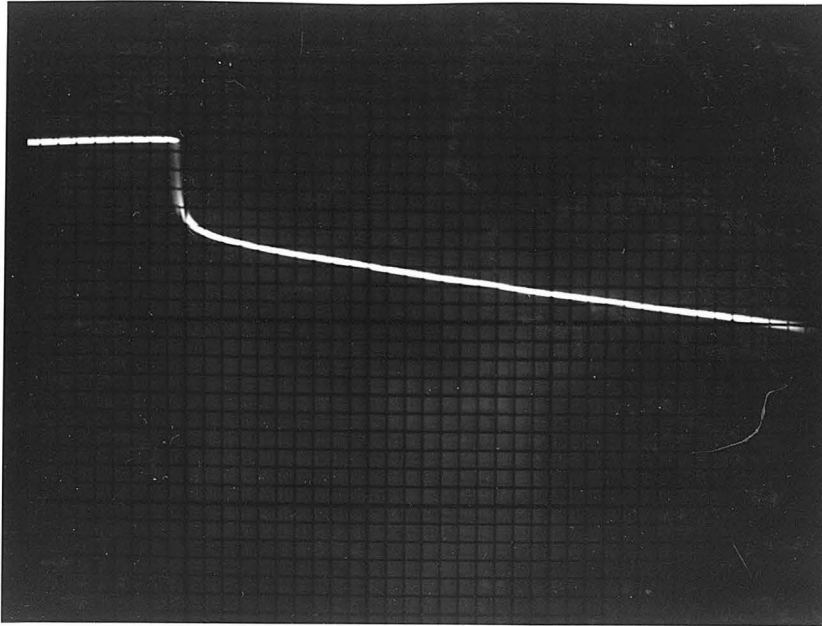


Figure 12. Typical oscilloscope photograph

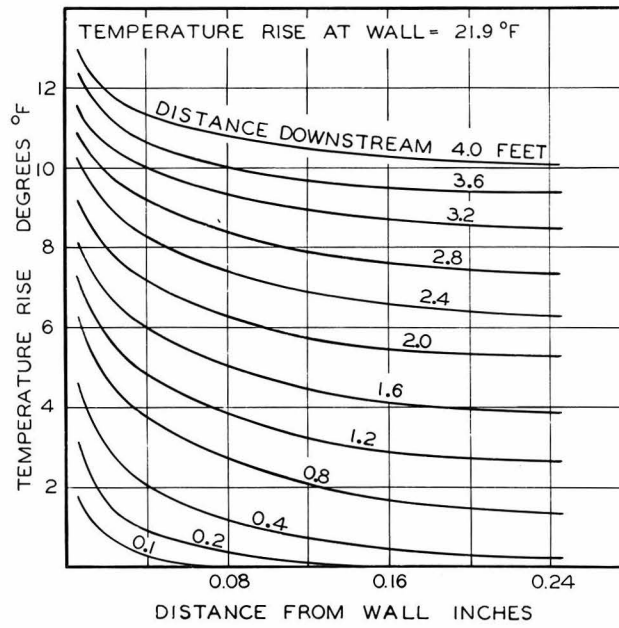


Figure 13. Temperature distribution Case A.

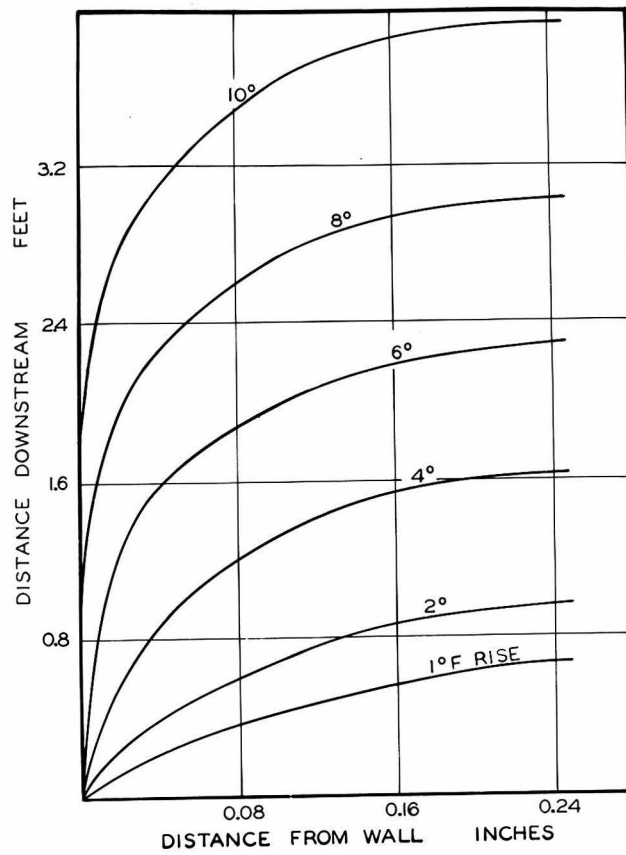


Figure 14. Curves of constant temperature
Case A.

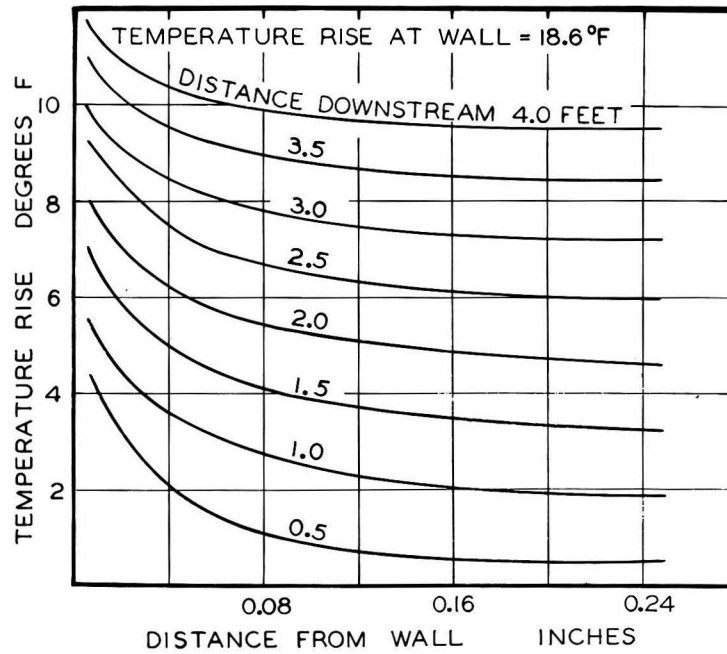


Figure 15. Temperature distribution
Case B.

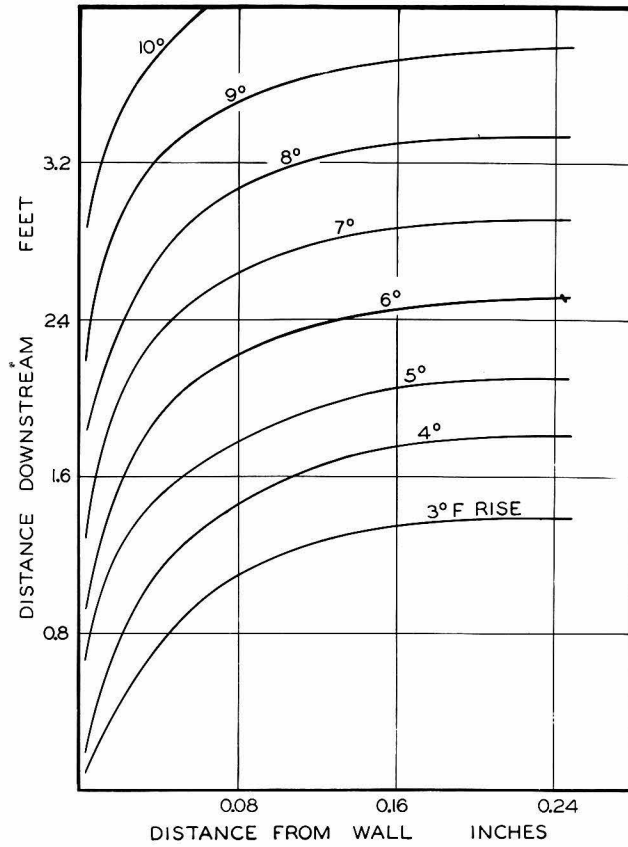


Figure 16. Curves of constant temperature
Case B.

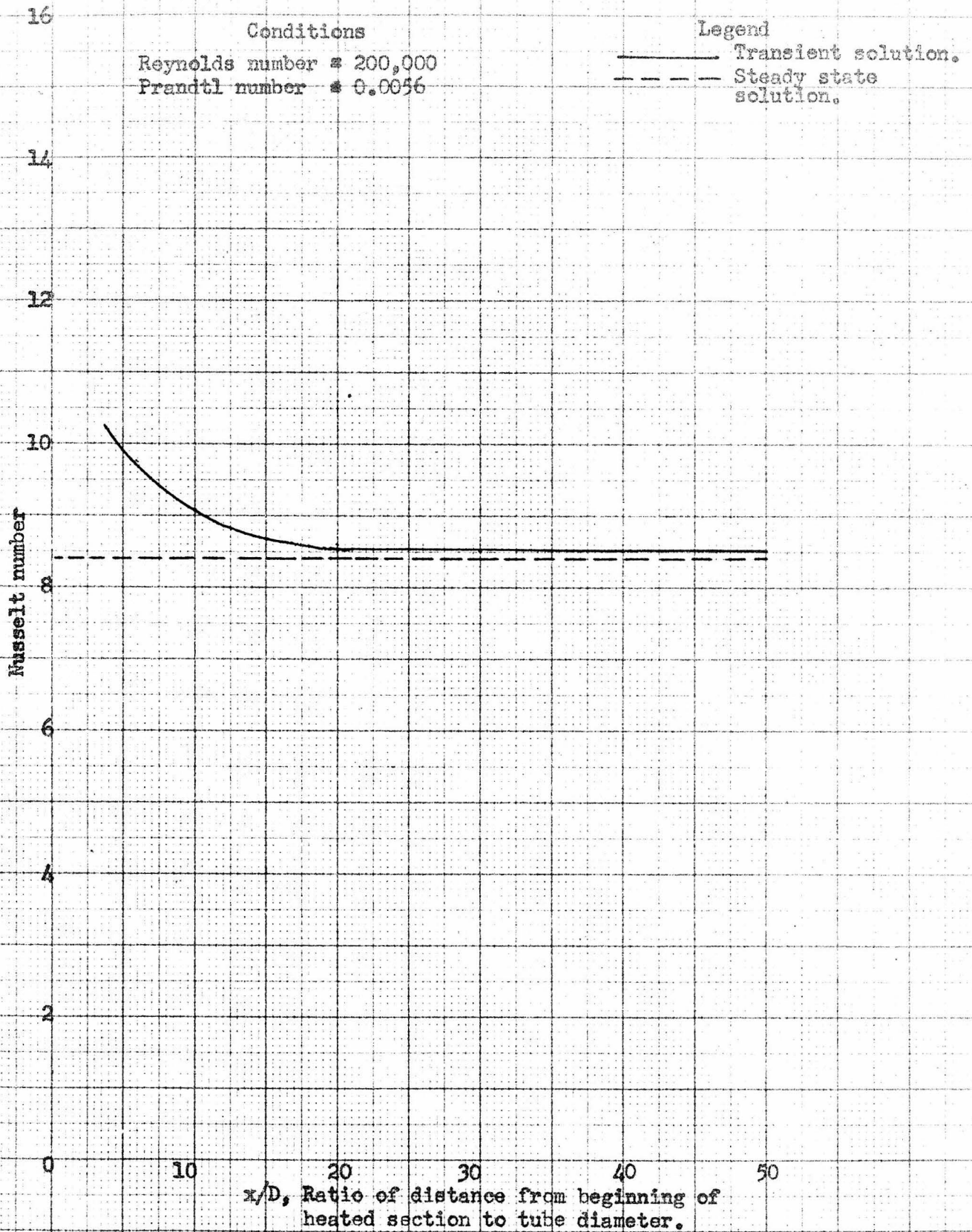


Figure 17. Nusselt number calculated for heating of mercury.

	Low Prandtl number, < 0.1 (liquid metals)	Medium Prandtl number, $0.1 - 1.0$ (gases, water, light liquids)	High Prandtl number > 10 (Heavy oils, glycerin, etc.)
Location of major resistance to heat flow	Turbulent core	Laminar layer, buffer layer, and turbulent core are all important	Laminar layer
Influence of velocity distribution assumed near the tube wall	Negligible	Medium	Large
Influence of ratio on calculated heat transfer	Large	Medium	Small
Effect of length to diameter ratio on heat transfer	Appreciable for first ten tube diameters after heating begins	Appreciable for first twenty tube diameters	
Variation of fluid properties with temperature	Small	Medium	Large

Figure 18. Factors influencing heat transfer inside tubes as a function of Prandtl modulus.

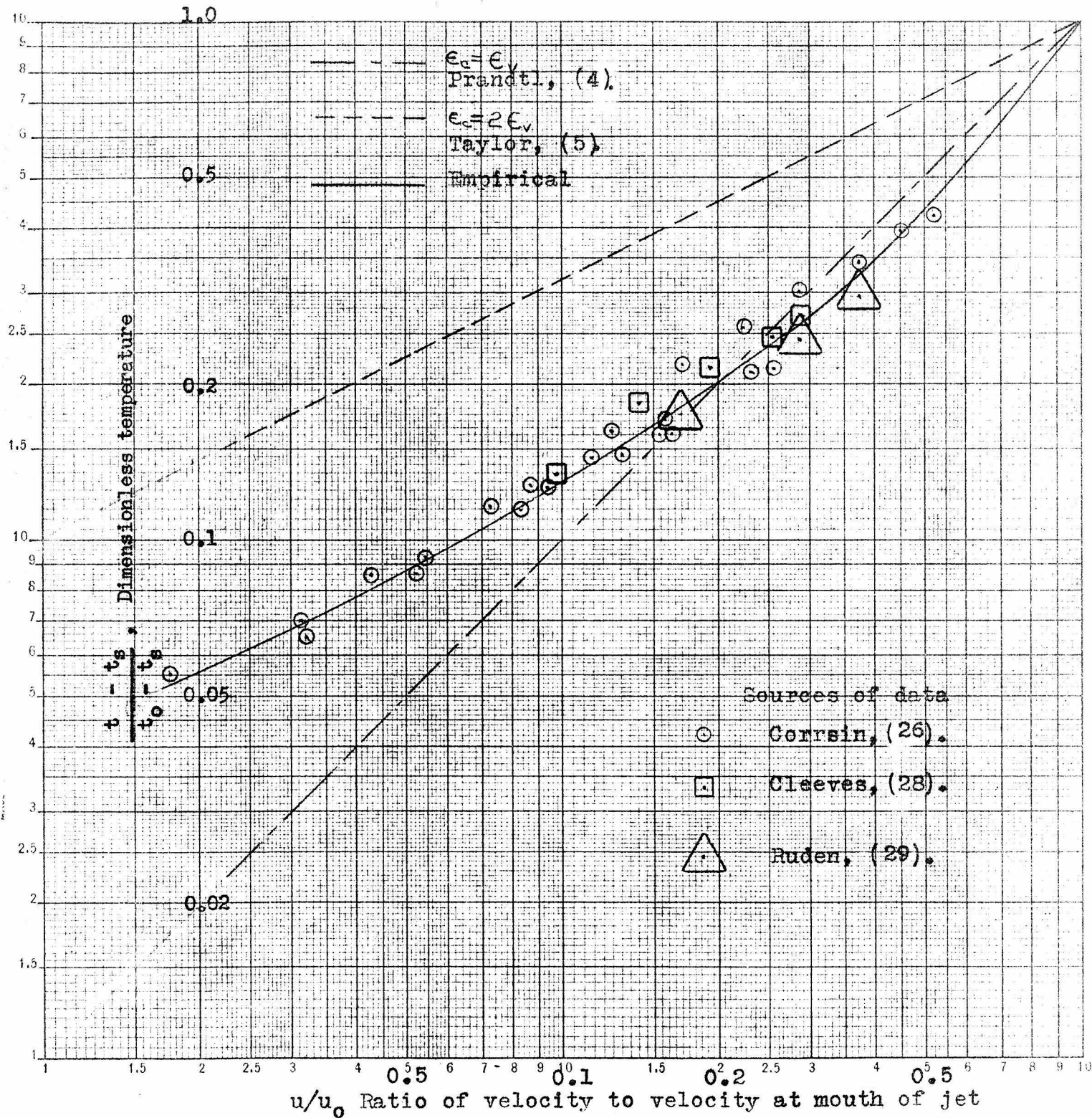


Figure 19. Temperature distribution in heated jets.

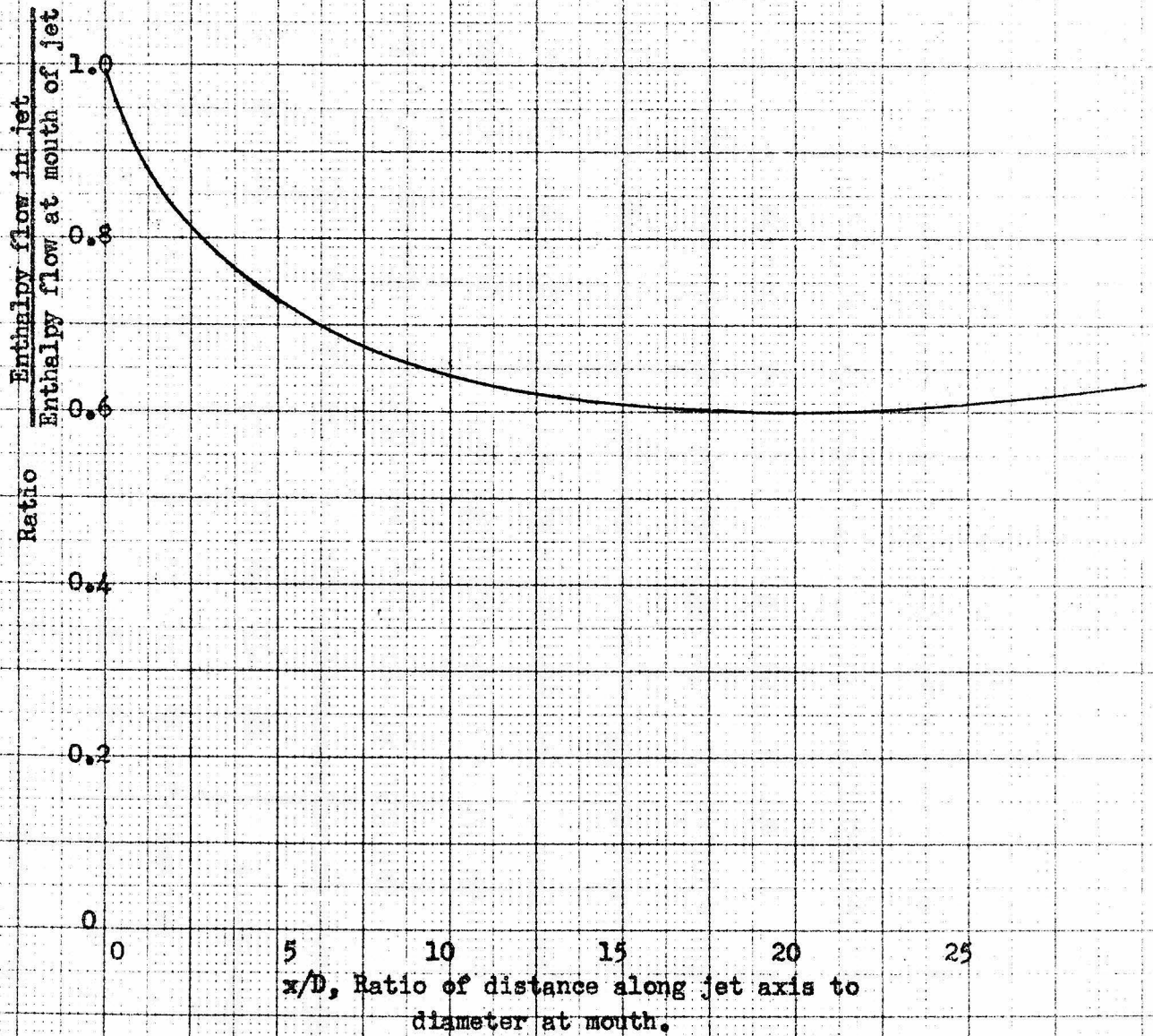


Figure 20. Enthalpy flow in a heated air jet.

Part II

An Attempt to Measure the Eddy

Diffusivity in Uniform

Turbulent Flow

RADIATION MEASUREMENT

The greatest effort in performance of these experiments has been devoted to the development of an instrument capable of measuring accurately the weak intensities of radiation employed. The isotope used is iodine - 131, which has a half-life of 8.0 days, emitting gamma rays, and beta rays which have a maximum energy of 0.67 million electron volts, (1). It has been decided that in order to avoid serious radiation hazards, a maximum of 20 millicuries of this isotope will be used at any one time.

In a preliminary experiment on the use of this method, in which 5 millicuries of radioactive iodoform were evaporated in the heat transfer apparatus, the volume of air carrying away the iodoform was approximately 10^6 as large as the volume of one of the samples used for measurement, at the lowest air velocity which could be used. At the highest velocities used for heat transfer measurements, this factor would become 2×10^7 . This unusually large dilution ratio was the entire justification for use of a tracer technique, but made it necessary to use a counter tube that will record 5-10% of the disintegrations occurring in a 100 cc gas sample.

Several types of instruments listed below, have been given detailed consideration for this application.

1. Thin-walled glass Geiger tube sealed in a concentric glass jacket, shown in Figure 1.
2. Six thin-walled, aluminum Geiger tubes sealed in a stainless steel chamber, shown in Figures 2 and 3.
3. Glass Geiger tube, adapted to count air samples introduced internally, shown in Figure 4.
4. Lauritsen quartz fiber electroscope, adapted for internal air sample.
5. Two large, end window Geiger tubes, with the thin ends forming a chamber for the active gas.

With the exception of the Lauritsen electroscope, all of these methods have been given active trials. Measurements on samples of active iodoform vapor of known relative concentration have shown that tubes of type 1 yield results of adequate precision, but are insufficiently sensitive. An instrument of type 2 has shown fair counting characteristics, and is expected to be entirely satisfactory, since it was designed to give several times minimum necessary sensitivity.

The other possibilities listed were found unsuitable for this purpose. Since the preparation of Geiger counter tubes is still very much an art, brief descriptions of work on these latter instruments will be included.

The conventional Geiger counter consists of a thin

metal wire anode supported inside a cylindrical metal cathode. The volume between these electrodes is filled with a gas, frequently a mixture of 90% argon and 10% ethyl alcohol at a pressure of 10 cm. mercury. The anode is maintained at a high potential, of the order of 1000 volts. A sudden (10 microseconds) fall in voltage on the center wire is produced when a free electron is liberated inside the metal cylinder. Recording these voltage drops provides a means of counting the number of ionizing particles which enter the tube.

Type 1

Several tubes of this type were constructed and tested. A curve of counting rate as a function of voltage for a fixed sample, taken on one of them, is shown in Figure 5. Most Geiger counters used for quantitative work have a region in which counting rate is nearly independent of voltage. Such a region is found on this curve, and in it, the number of counts registered is equal to the number of ionizing particles passing through the sensitive part of the tube. Therefore, when the tube is operated at a voltage within the "plateau" of the curve, its rate of counting will be directly proportional to the concentration of radioactive iodoform vapor in the glass jacket.

This method was first tried by attaching glass sample

chambers to commercial counters with wax seals. Permanent contamination resulted from absorption of iodoform in the wax. Satisfactory operation was not obtained until all organic materials were eliminated by constructing the tubes described below.

In preparing these counters, the thin-walled, interior cylinder was first drawn, and a ground wire inserted through a side arm.

The jacket was prepared, with its stopcock attached, and then joined to the other piece with ring seals. The lower end of this inside tube was temporarily sealed off. The interior of this section in some of the counters was then chemically silvered throughout by means of the Rochelle salt process, described by Strong, (2). Any unwanted silver coating was removed by wiping lightly with a cloth. The Geiger tube on the left of Figure 1 has a silver surface of this type.

It was found that the interior face of this coating had a dull gray appearance. In an attempt to obtain a surface of lower photoelectric efficiency, one tube, shown on the right in Figure 1, was coated instead with "Liquid Bright Gold" solution, and baked. An unusually shiny interior face was produced. However, the counter~~ing~~ characteristics of this tube were not appreciably different from those which were silvered.

After application of the cathode surface, a glass tube was attached for filling, and the center wire was inserted by means of tungsten metal - to - glass seals at the ends of the interior tube, in which the actual counting took place. The active section of this anode consisted of 0.004 inch tungsten wire, drawn tight when the last seal was made.

All tubes were filled with the standard mixture of 90% argon and 10% absolute ethyl alcohol to a total pressure of 10 cm. of mercury. They were not baked out nor was the center wire glowed, both of which procedures are sometimes practiced.

An experiment was performed to verify directly the proportionality between counting rate registered by the Geiger tubes and concentration of active iodoform in the jacket. One of these counters was sealed into a vacuum system exposing only glass and metal surfaces to vapors transferred through it. A 1/4 gram, 10 millicurie, sample of active iodoform was allowed to vaporize in an air-filled, 5-gallon bottle. After allowing time for saturation to occur, this air was transferred into a 5-gallon bottle which had been evacuated to approximately 300 millimeters of mercury absolute pressure to separate it from the remaining solid iodoform.

Several hours were then allowed for uniformity of

composition to be reached. Portions of this mixture were then admitted to the jacket surrounding the counter, randomly varying pressures. Before entry of a given sample, the preceding one was removed completely by evacuation. Each time, the pressure of the air being counted was determined with a mercury manometer and a vertical component cathetometer. The temperature of the Geiger tube was recorded during each measurement, and all manometer readings were converted to pressure at 20° C. Since some series of measurements lasted as much as 12 hours, all counting rates were corrected for decay of the 8 day half-life iodine.

The results of three such series of measurements are shown in Figures 6, 7, and 8. The data plotted are given in Table I of the Appendix. During the first two runs, it was observed that the high voltage output of the counter circuit was unstable, having variations of 25 to 50 volts, this fluctuation was quite serious. The trouble was eliminated by operating this power supply with an input of 125 volts, instead of the usual 110 volts.

The last data shown which are in Figure 8, were obtained under this condition. The number of counts taken at each point varied from 1000 to 3000, with an average of 2200.

If all the counts recorded are produced by disinte-

gration of an iodine nucleus, their occurrence will be mutually independent. On this basis, it has been shown, (3), that the standard deviation of a single observation is given by the formula

$$\text{Deviation} = (N)^{-\frac{1}{2}}$$

providing no other uncertainties are present, where N is the number of counts taken.

For the points in the last run, this deviation varied from 16% to 45%. The predicted standard deviation of the entire set of measurements was 2%, while that calculated from the observed counting rates was 2½%. In consideration of this deviation, it is believed that the precision provided by this method of analysis is entirely adequate for studies of turbulent diffusion.

An attempt was made to use this type of Geiger tube for an actual determination of diffusion rates above a surface of iodoform in the air stream of the heat transfer apparatus. The concentration of the iodoform in the samples taken was so much less than those previously used that the activity observed was less than one quarter of the background, making quantitative measurement impossible.

The more sensitive counter described below was constructed in the hope of eliminating this difficulty.

Type 2

Two types of losses in sensitivity are present in radiation measurement. First is absorption or deflection of the particles or light quanta before they reach the sensitive portion of the measuring instrument. Second is geometrical factor, represented by the available solid angle of the counter.

The average thickness in the sensitive area of the Geiger tube used in run on the heat transfer apparatus was 0.00863 inches, or 57.5 mg./cm². From the curve shown in Figure 9, this corresponds to transmission of only 17.5% of the radiation. An approximate equation for the fraction of the radiation reaching the exterior of the sensitive section, called F, has been derived for the configuration of type 1, and is presented below.

$$F = \left(\frac{l}{L} \right) \frac{r_1(r_2 - r_1)}{r_2^2} \quad (2)$$

l and L are the lengths of the sensitive section and the jacket, respectively, while r₁ and r₂ are the inner and outer radii of the glass tubes. The numerical value of F is about 8%, from which the overall fraction of the disintegrations recorded was 1.4%.

The new counter designed to remedy this difficulty is shown in Figures 2 and 3. The six Geiger tubes form a

ring enclosing a large fraction of the volume of the stainless steel chamber. The aluminum walls of the counters are machine made, and it is expected that a reproducible thickness has been achieved. Their weight is specified by the manufacturer to be 30 mg/cm^2 , which corresponds to 39% transmission of the radiation.

Using equation 5 (g), p. 54, in McAdams' "Heat Transmission", (4), the geometrical efficiency of this new counter has been estimated at 35-40%. From this value, the overall efficiency of the assembly is calculated to be 15-16%, representing an improvement by a factor of ten.

The electrical characteristics of these tubes have proved to be satisfactory. A graph of counting rate as a function of voltage for a constant sample is shown in Figure 10. The points are as reproducible as the voltage settings on the high voltage supply.

In connecting this instrument, a 5 meg-ohm resistor has been introduced in series with each counter to reduce the effective capacitance present in firing of one of the tubes. Without them, the capacitance of all six counters would be in parallel; six times as much ionization would be produced in each pulse before the center-wire potential would reach the threshold value and recovery of the tube to its initial state could begin. This would mean a proportional increase in the number of "spurious" pulses, and shortening

in the useful life of the tubes.

The individual counters are sealed into the chamber by means of neoprene gaskets fitting under small flanges located near one end of the tube. A pressure of less than one micron is obtained regularly in this unit.

These Geiger Tubes were also tried in an attempt to measure eddy diffusivities in an air stream above a surface of radioactive iodoform. Again, the intensity of radiation was found to be very weak. In addition, a certain degree of contamination remained in the counter after each sample.

Types 3, 4, and 5

The most sensitive means of determining the intensity of beta radiation from a sample of gas is the introduction of this gas into the electric field of a Geiger counter. Then every nuclear disintegration occurring within the active region of this field will produce a count. This procedure has been employed in several instances, for measurement of concentrations of carbon - 14 and hydrogen - 3. Elaborate voltage regulation equipment was developed for this application by Brown, (5). The precision of this instrument was discussed, but no quantitative evaluation of its uncertainties was presented.

The gas of interest in this case was atmospheric air. Since any attempts to eliminate the dust or moisture con-

tent of this air might also remove the radioactive iodoform, the presence of these components could not be regulated.

Conflicting viewpoints have been expressed in the literature on the use of Geiger counters filled with gases containing free oxygen. Neher, (2), states that air at a pressure of 3 to 6 centimeters of mercury results in a satisfactory counter. Korff, (6), states that use of oxygen as a filling gas is undesirable due to formation of negative oxygen ions.

One of the tubes shown in Figure was connected so that air samples could be introduced inside the cathode volume. A Neher-Harper quenching circuit was attached to this counter in order to stop the flow of current after each pulse. Some device for this purpose is necessary whenever the filling gas does not contain several percent, or more, of a polyatomic vapor. Very erratic results were obtained from this arrangement, even when the voltage drop occurring in the pulses produced by the tube was kept constant for different samples by means of a cathode-ray oscilloscope.

Characteristics most like those of normal counters were obtained from the Geiger tube shown in Figure 4, by filling it with a mixture of 20% absolute ethanol and 80% air, to a total pressure of $6 \frac{1}{4}$ centimeters of mercury. A curve of counting rate versus voltage for a fixed activity source is given in Figure 15. No metal cathode is used in

this tube; the gold coating seen in the photograph is on the outside of the cylinder wall. Soft glass construction was used to allow dissipation of accumulated charge from the interior surface. This design is intended to reduce emission of photoelectrons from the cathode surface.

Consideration was given to use of the Lauritsen electroscope in this program because of the reliability and simplicity of this instrument. Henriques, et al, (7), have measured portions of carbon - 14, sulfur - 35, and hydrogen - 3, as small as the present iodine samples, with this tool. The higher energy of the beta radiation from iodine - 131 makes this technique unfavorable.

The reading of an electroscope is nearly proportional to the number of ion - pairs liberated within its chamber. Greater ionization per unit length of path is produced by low energy beta rays than by those of higher energy. The sensitivity of an electroscope to iodine - 131 would be roughly one-fifth that to carbon - 14.

Construction of two 3 inch diameter, mica window counters fitting into a sample chamber was attempted. Three inch brass pipe was used for the cathode walls. A large sheet of Indian ruby mica obtained from the Physics stockroom was split several times to yield a layer 15 - 20 mg./cm.² in weight (0.002 inches thick) which would withstand repeated application of a pressure difference of one

atmosphere over this 7 square inch area. Pulses were observed from the tube, but response was highly erratic, and a leak was developed after approximately 25 fillings with argon alcohol mixture.

The Heat Transfer Apparatus

The equipment used for the experiments on eddy diffusion thus far performed, and to be used for those proposed is the heat transfer apparatus of the Chemical Engineering department. This apparatus is described in detail by Corcoran, (10). Some of the pertinent features are discussed below.

A photograph of the equipment as used for this program is shown in Figure 11. In the working section, the air flows between two parallel copper plates, in a channel 0.75 inches high, 12 3/8 inches wide and 162 inches in length. A rectangular duct has been installed in the system downstream of the working section to dispose of air containing radioactive iodoform vapor when material transfer measurements are in progress. Adjacent to the copper plates are two oil baths, which permit their temperatures to be controlled to within 0.005° F. A direct heater permits the air temperature to be controlled with the same precision.

Traversing gear installed on this equipment permits velocities and temperatures to be determined, and samples of

the air to be taken at any point within the channel. This is shown in Figure 12.

These samples are withdrawn through the pitot tube used for velocity measurement, which has an outside diameter of 0.030 inch. The position of its center-line may be measured to within 0.0005 inch. A drawing of this sample tube, with a hot-wire anemometer, as located in the air channel, is shown in Figure 13. Measurements of air velocity, which are necessary for calculation of the eddy diffusivity, may be taken with a hot-wire anemometer in addition to the pitot tube. The uncertainty is in both cases 0.1-0.4 ft/sec, depending on velocity.

Portable Analysis Unit

In order to withdraw samples rapidly from a flowing gas stream and analyze them as an experiment is being performed, special apparatus was constructed. A photograph of the complete assembly is shown in Figure 14.

A vacuum system was provided so that a sample could be drawn directly into an evacuated chamber around a Geiger counter (or group of counters) to measure its intensity of radiation.

The possibility of continuously drawing the gas past a counting chamber was considered, but the volume of flow necessary to achieve steady state would be order - of -

magnitude larger, and the sample pressure could not be so readily controlled.

A mercury manometer was provided for measurement of pressure within the vacuum manifold and the counting chamber. In order to secure rapid, thorough evacuation of the system, both a mercury diffusion pump and a Cenco Hyvac pump were installed on the movable bench. One novel feature of the apparatus is the means of cooling the diffusion pump. The water from the condenser is passed through a length of copper tubing which is soldered under the lower aluminum plate, providing sufficient area to dissipate the heat to the atmosphere. A McLeod gauge, operated by a leveling bulb, is attached directly to the vacuum manifold. With the present Geiger counter tubes installed, a pressure of less than 1 micron was routinely obtained.

A rotameter and an extension of copper tubing is provided to connect the glass system with the pitot tube of the heat transfer apparatus. Use of the rotameter permits measurement of the rate of withdrawal of the samples, while presenting a minimum obstruction to their flow, so that the velocity of air entering the pitot tube may be kept below the velocity of the stream approaching the pitot tube. The rotameter was calibrated after installation by means of a wet test meter. By plugging the end of the pitot tube the entire line was checked and found free of vacuum leaks.

A lead shield enclosing the Geiger counter tubes, a counting circuit, and a timer connected to the scaling circuit are installed permanently on the upper level.

This group of equipment was assembled on a portable bench so that it could be removed from the operating area when heat transfer measurements were being taken.

Preparation And Deposition Of Iodoform

The radioactive iodine used in this investigation was obtained from the Atomic Energy Commission in the form of a carrier free solution of sodium iodide in distilled water. The 20 millicurie shipments were shipped in approximately 3 c.c. of solution.

Active iodoform was prepared from this material in the special isotopes laboratory at this Institute. The most satisfactory procedure developed was the addition of sodium hypochlorite solution to a mixture of acetone, sodium hydroxide, carrier sodium iodide, and the iodine - 131 solution. The equation for the reaction involved is



The quantities used in this preparation were: 1.00 gms. NaI, 6.00 c.c. of 16% NaOCl solution and 0.129 gms. of acetone, and 10 c.c. of distilled water. The sodium iodide was first weighed out into a 50 c.c. centrifuge tube. The radioactive iodine solution was then added, its container being washed out by means of the additional water. The acetone was added as a 20% by volume solution in water to facilitate measurement of the quantity used. Finally, the sodium hypochlorite solution was introduced drop by drop, with mechanical stirring.

The solid iodoform was precipitated immediately during this last addition, and separated from the supernatant liquid by centrifuging and decanting. Ten c.c. of absolute alcohol were added, and the centrifuge tube was heated in a water bath to dissolve the precipitate. This iodoform was then recrystallized from the solution by cooling in dry ice-acetone mixture. Measurement of the radiation from this precipitate by means of the Chemistry Department radiation monitor indicated 60-70% recovery of the iodine - 131, the quantity varying slightly from one preparation to the next.

Attempts were made to synthesize the iodoform using potassium persulfate as an oxidizing agent, instead of sodium hypochlorite, and also by means of an electrolytic method. Neither of these proved satisfactory.

The deposition of a uniform coating of iodoform on the lower copper plate offered certain inherent difficulties. As previously mentioned, the height of the air channel above this plate is only 0.75 inch.

It was originally intended to attach a metal dam to this surface in order to hold a solution of iodoform in an organic solvent over the area while the liquid evaporated. Experiments on this technique showed that a satisfactory coating could be produced. However, it was discovered that the air channel deviated sufficiently from a horizontal plane to cause the evaporation solution to run entirely to one edge of the area and produce uneven precipitation.

Coatings produced by spraying solutions of iodoform in alcohol and acetone proved to be quite uniform in appearance. A sprayer which could be used in the restricted space available was constructed.

A section of 1/16 inch stainless steel tubing was silver soldered to a 3 foot length of 3/8 inch brass tubing closed at one end. A 1/16 inch hole was drilled in the large tubing at the end point of the small tube. The sprayer was used by inserting the free end of the stainless steel tube into a centrifuge tube containing iodoform solution, and blowing air through the 1/16 inch hole, thereby drawing up and dispersing the liquid. The portion of the air channel not sprayed was masked off with kraft paper.

The writer and other workers in this laboratory originally feared that the lower copper plate of the heat transfer apparatus might be corroded by the iodoform to be coated on the surface. Repeated tests on a sample copper sheet demonstrated that no corrosion was produced when iodoform which had been freshly prepared or recrystallized was used.

Discussion

After the second unsuccessful attempt to obtain measurements of iodoform concentration in the air channel, a list of possible explanations for the lack of results was examined. Since the

Geiger counter tubes were tested immediately before and after the run, they are assumed to have been operating. Previously, many tests had been made in which iodoform samples were drawn into a counter from a bottle containing solid iodoform. No evidence of loss of the iodoform in the sampling lines was found.

The fact that most of the radioactive iodine arriving at the institute from the Atomic Energy Commission reached the heat transfer apparatus had been verified on the previous run by use of a laboratory monitor. Measurements were made around the apparatus after the last run with an exposed Geiger tube from the assembly shown in Figure 3. Only a very small fraction of the radiation which originally had been present remained. This verified the assumption that the radioactivity left the area on which it was deposited while the air stream was flowing.

The number of disintegrations per unit volume of air which would have been obtained if the iodoform had evaporated was calculated. The counting rate which was expected at this

concentration of radioactive vapor was calculated from the efficiency previously estimated for this counter. The result was greater than the observed counting rate by a factor of more than 100. It was then concluded that the iodoform had blown away, instead of evaporating.

NOMENCLATURE

C	Concentration, lbs/ft ³
D	Diffusion coefficient, ft ² /sec
F	Fraction of radiation for air sample reaching exterior of sensitive portion of Geiger counter
l	Length of sensitive section of Geiger tube
L	Length of jacket of Geiger tube
M	Rate of material transfer, lbs/ft ² sec
r ₁	Inner radius of annular sample chamber
r ₂	Outer radius of annular sample chamber
D	Eddy diffusivity, ft ² /sec

REFERENCES

1. J. Downing, M. Deutsch, and A. Roberts, Phys. Rev., 61, 389, 686, (1942).
2. J. Strong, "Procedures in Experimental Physics," 157, 269, Prentice-Hall, (1938).
3. Wein-Harns, "Handbuch der Experimental Physik," XV, 786, Leipzig (1928).
4. W. H. McAdams, "Heat Transmission," Second Edition, McGraw Hill Book Co., New York, (1942)
5. S. C. Brown, W. M. Good, and R. D. Evans, Rev. Sci. Inst. 16, 125, (1945).
6. S. A. Korff, "Electron and Nuclear Counters," p. 80, D. Van Nostrand Co., New York, (1946).
7. E. C. Henriques, Ind. Eng. Chem., and Ed., 18, 349, 415, 417, 420, (1946).
8. W. H. Corcoran, Ph.D. Thesis, California Institute of Technology, (1948).

TABLE I

Rate of Counting as a Function of Sample Pressure

Run I Shown in Figure		Run II Shown in Figure	
Counts Per Second	Sample Pressure	Counts Per Second	Sample Pressure
0.90	0	0.669	0
7.73	45.1	2.29	18.33
2.38	9.6	0.610	0
5.47	25.5	8.01	53.6
6.91	33.6	4.52	29.7
8.20	41.3	0.645	0
4.68	19.8	9.15	58.6
8.39	40.9	6.07	38.2
5.28	25.3	6.09	37.3
3.59	14.3	8.79	55.6
2.41	8.1	8.05	49.9
5.64	29.4	4.20	23.1
5.99	32.2	7.95	52.4
5.45	26.7	4.31	24.8
3.08	11.6	0.678	0
1.63	7.5	7.70	45.5
0.75	0	1.94	6.8
5.49	2.57	7.63	46.1
		7.99	47.7
		2.90	15.5

Run III
Shown in Figure 8

Counts Per Second	Sample Pressure
2.98	17.9
4.48	29.8
3.11	19.55
5.09	33.2
0.64	0
0.68	0
6.14	42.9
6.62	45.4
4.36	29.9
5.67	39.2
4.18	36.4
4.18	29.2
5.64	39.7
2.49	14.74
3.47	22.0
5.62	40.0
5.01	34.6
4.49	31.8
0.57	0
2.09	11.9
5.47	37.8
2.79	15.74
3.90	25.8
3.57	22.2

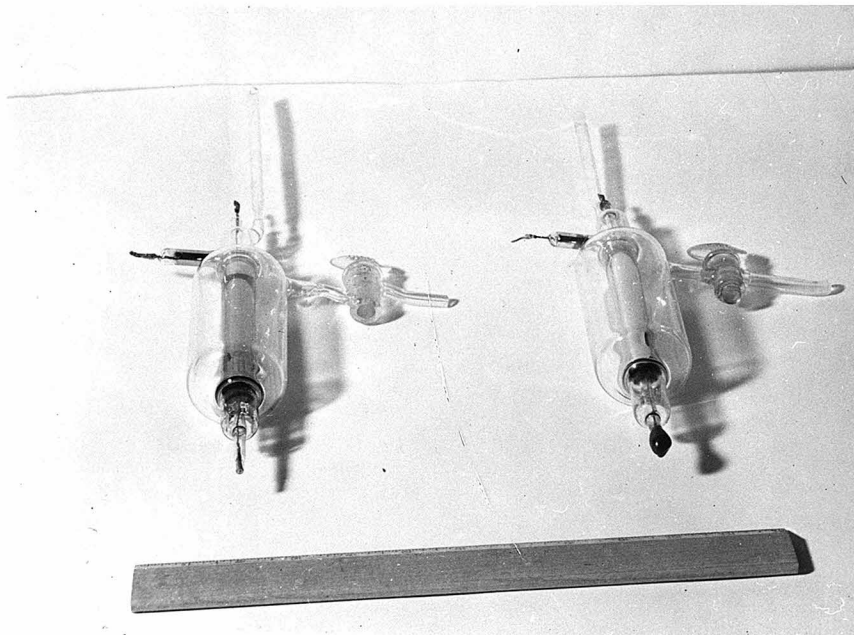


Figure 1.

Glass Geiger counter tubes
with concentric jackets

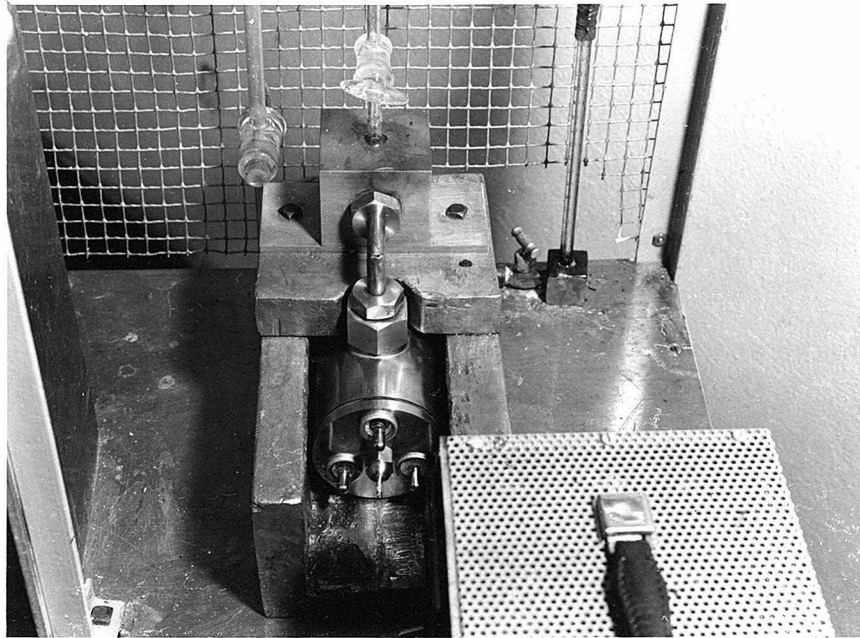


Figure 2

Aluminum Geiger counter tubes
in stainless steel chamber

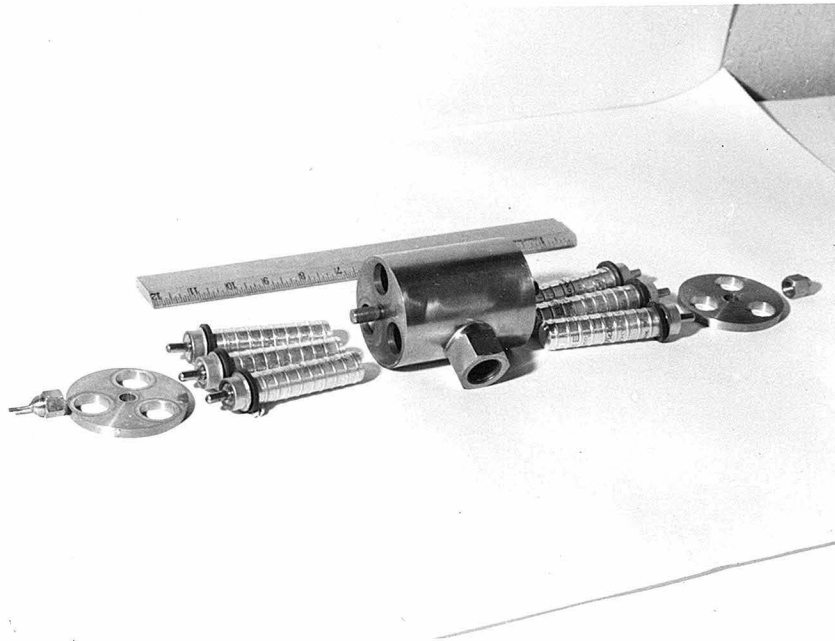


Figure 3

**Exploded view of aluminum Geiger
counter assembly**

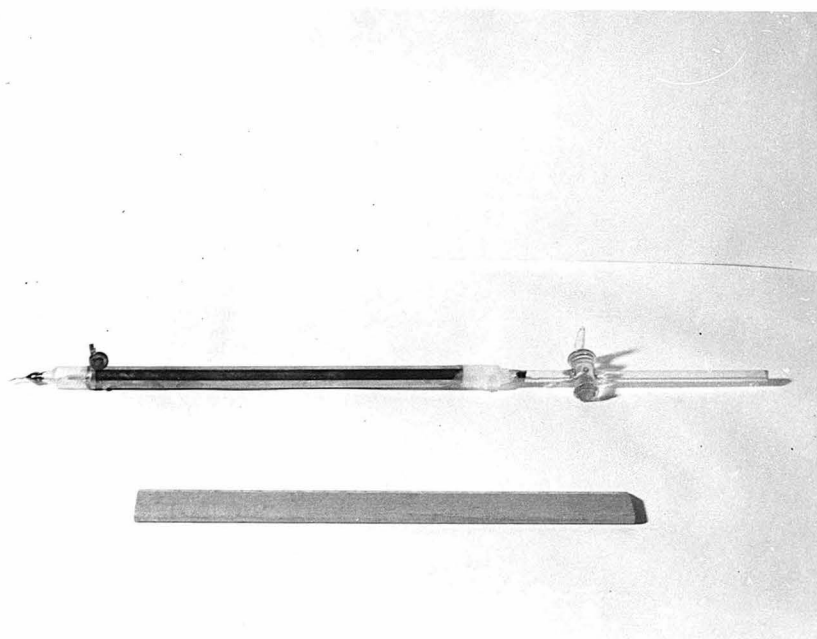
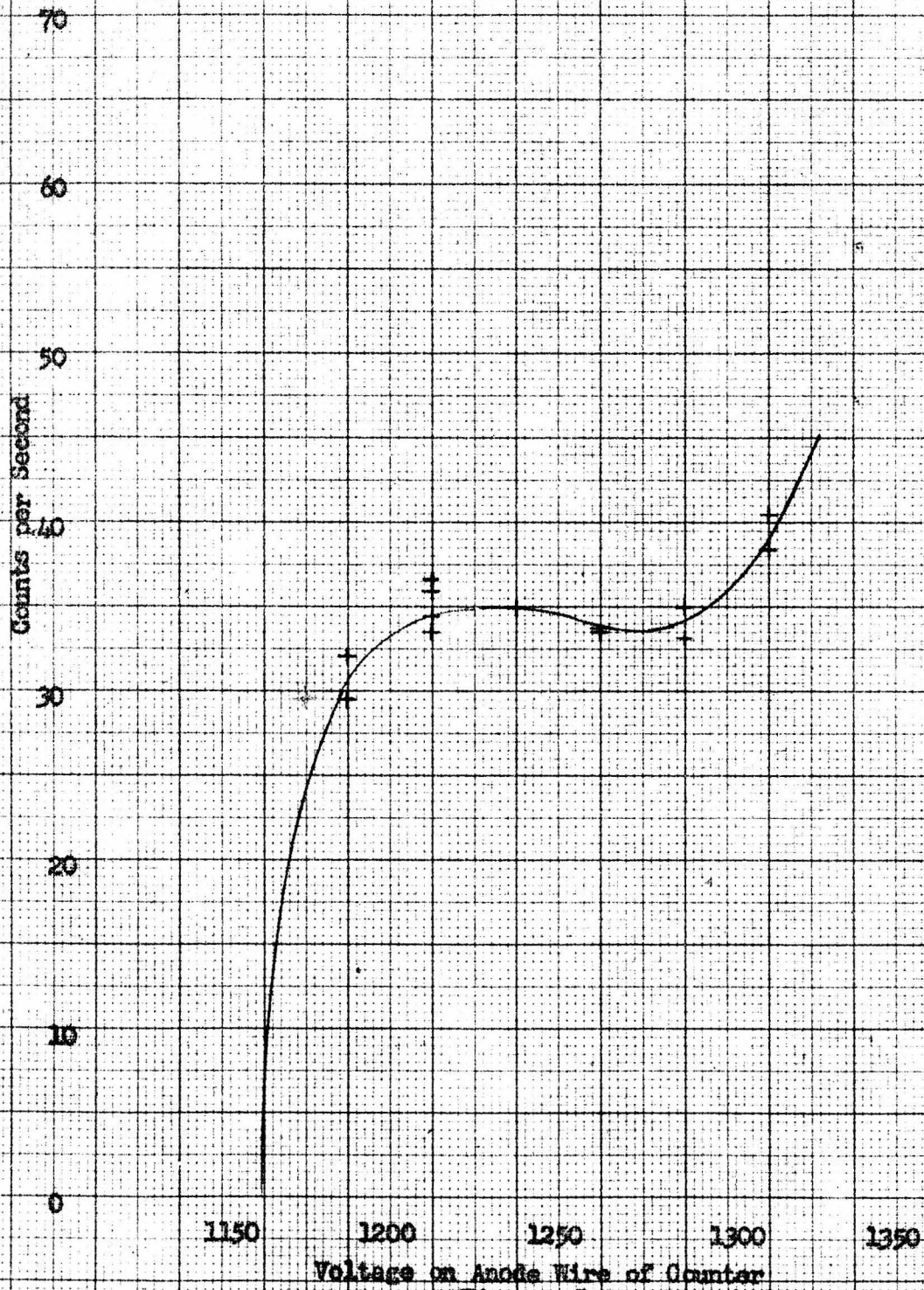


Figure 4

Geiger counter tube for
internal gas sample

Observed rate of Counting as a
Function of Voltage for
a Fixed Sample
Type I Geiger Tube



Voltage on Anode Wire of Counter
Figure 5

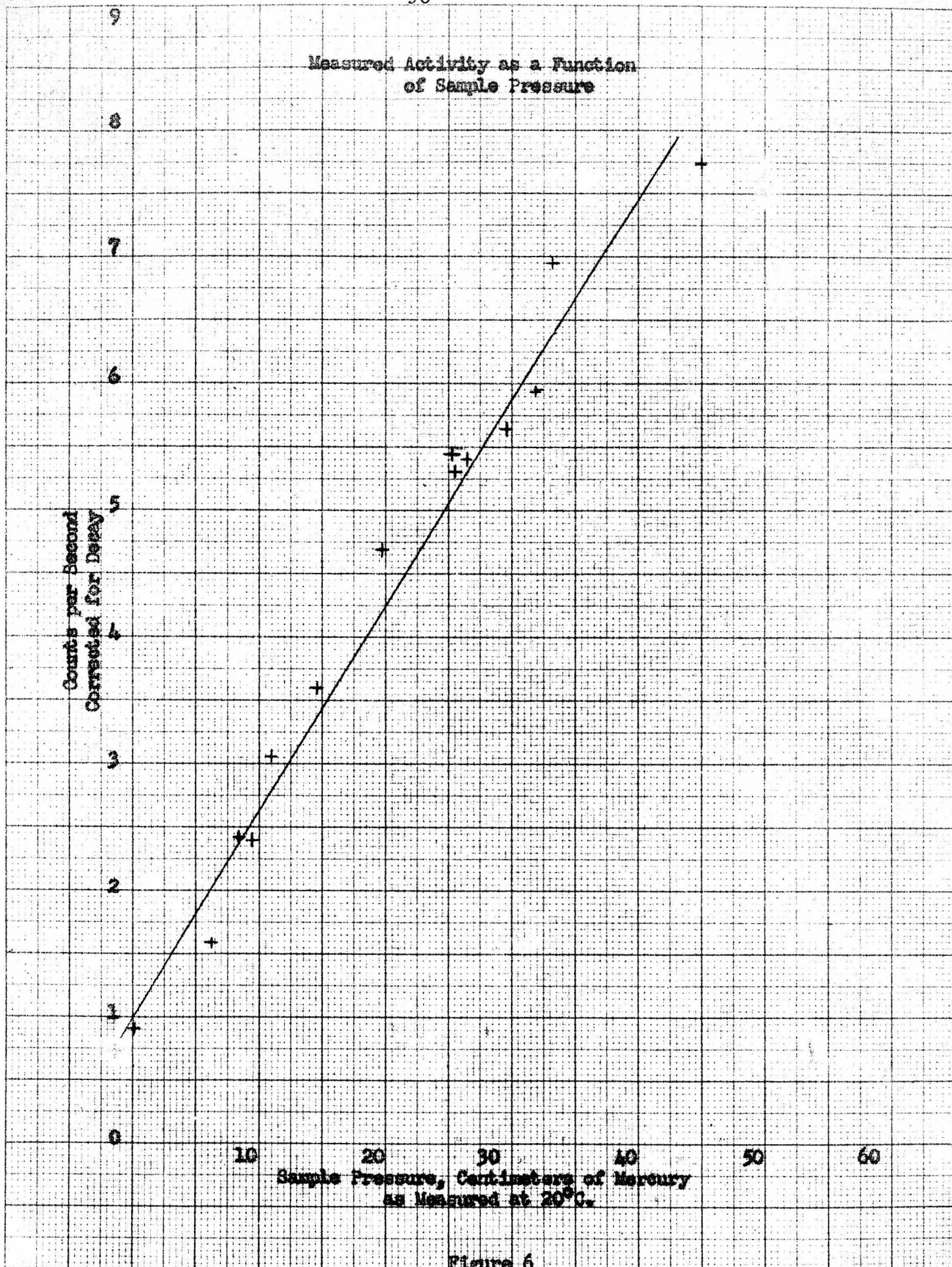


Figure 6

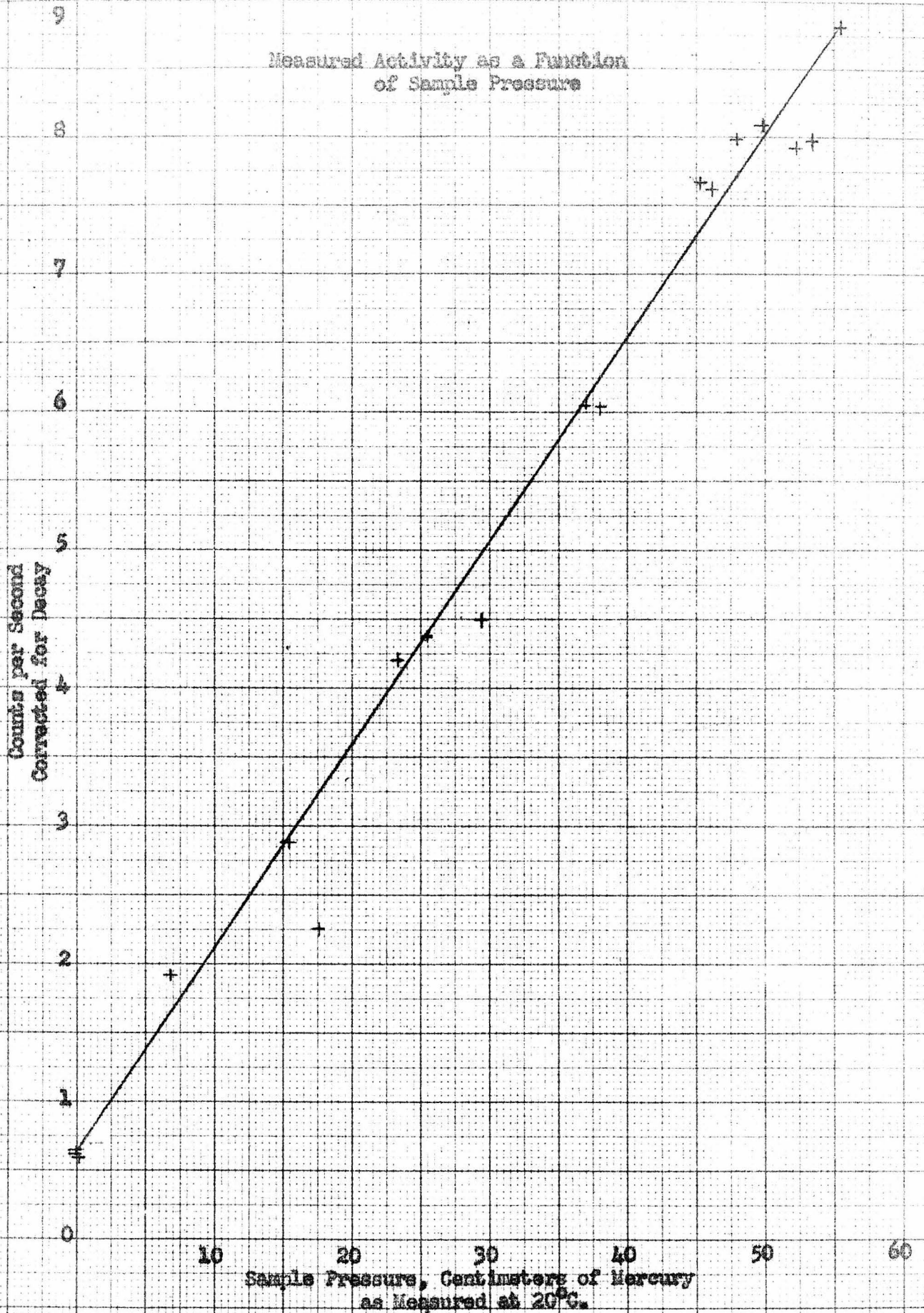


Figure 7

Measured Activity as a Function
of Sample Pressure

Counts per Second
Corrected for Decay

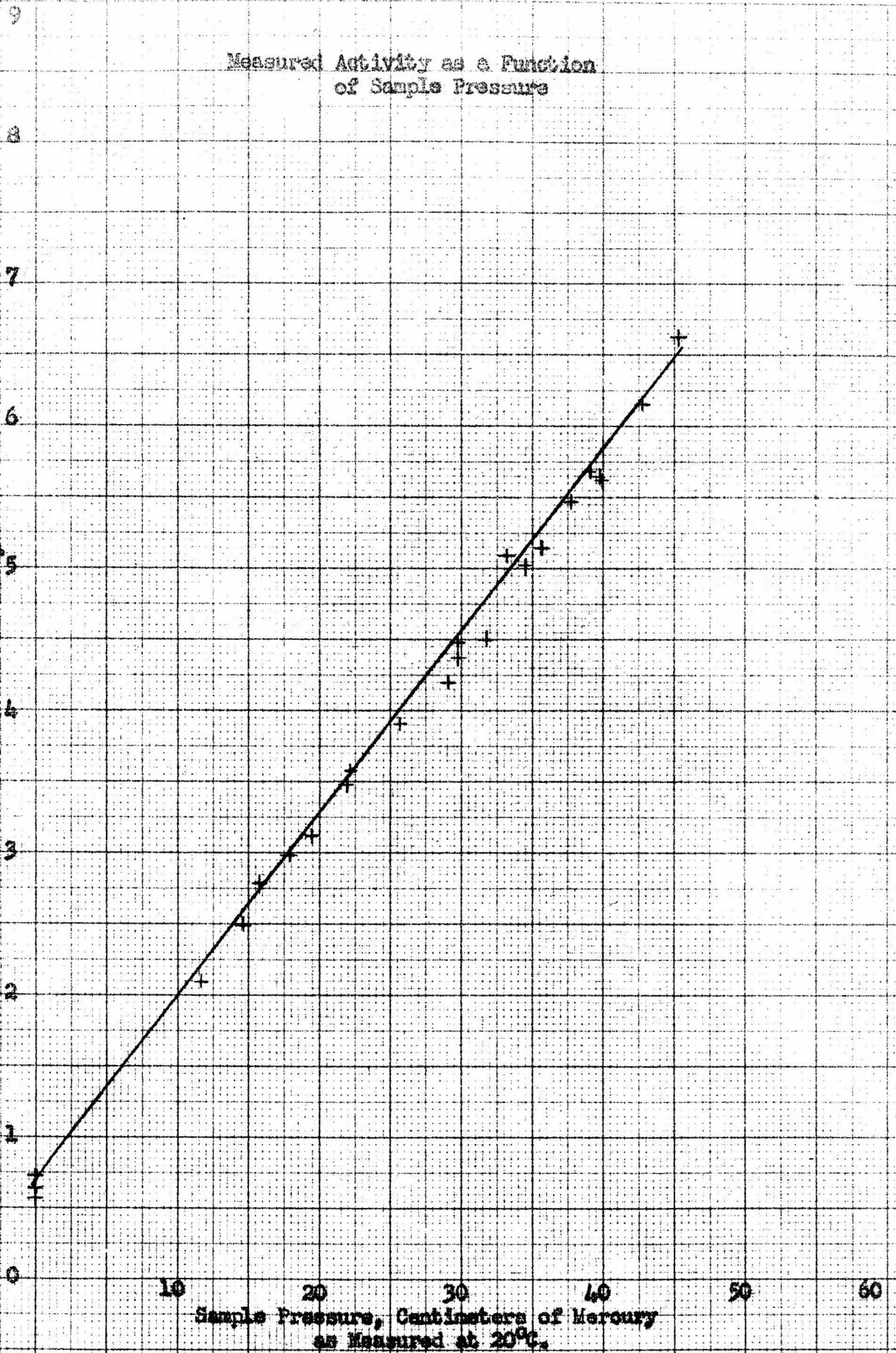


Figure 8

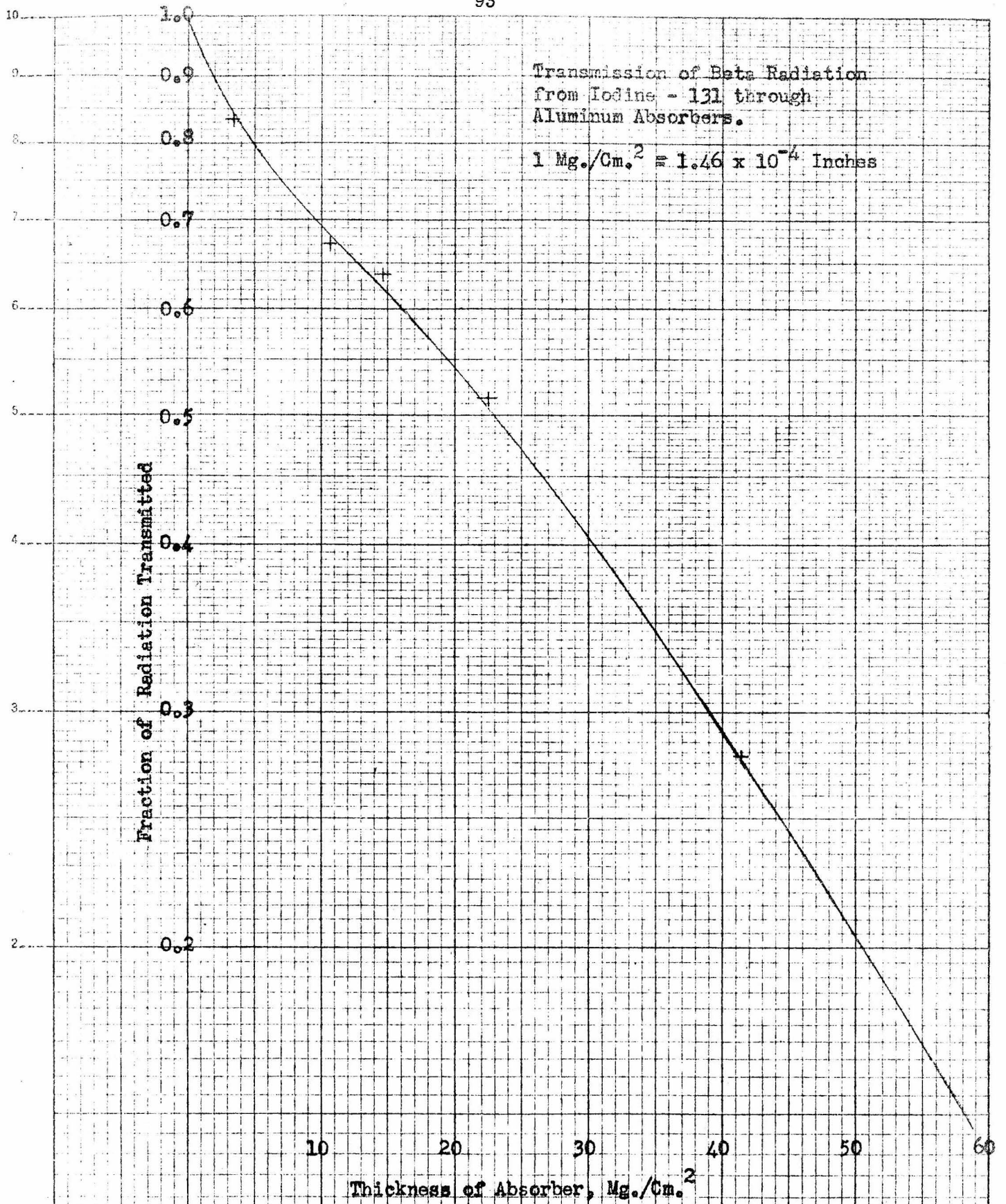


Figure 9

Observed Rate of Counting as a
Function of Voltage for
a Fixed Sample

Type 2 Geiger Tube

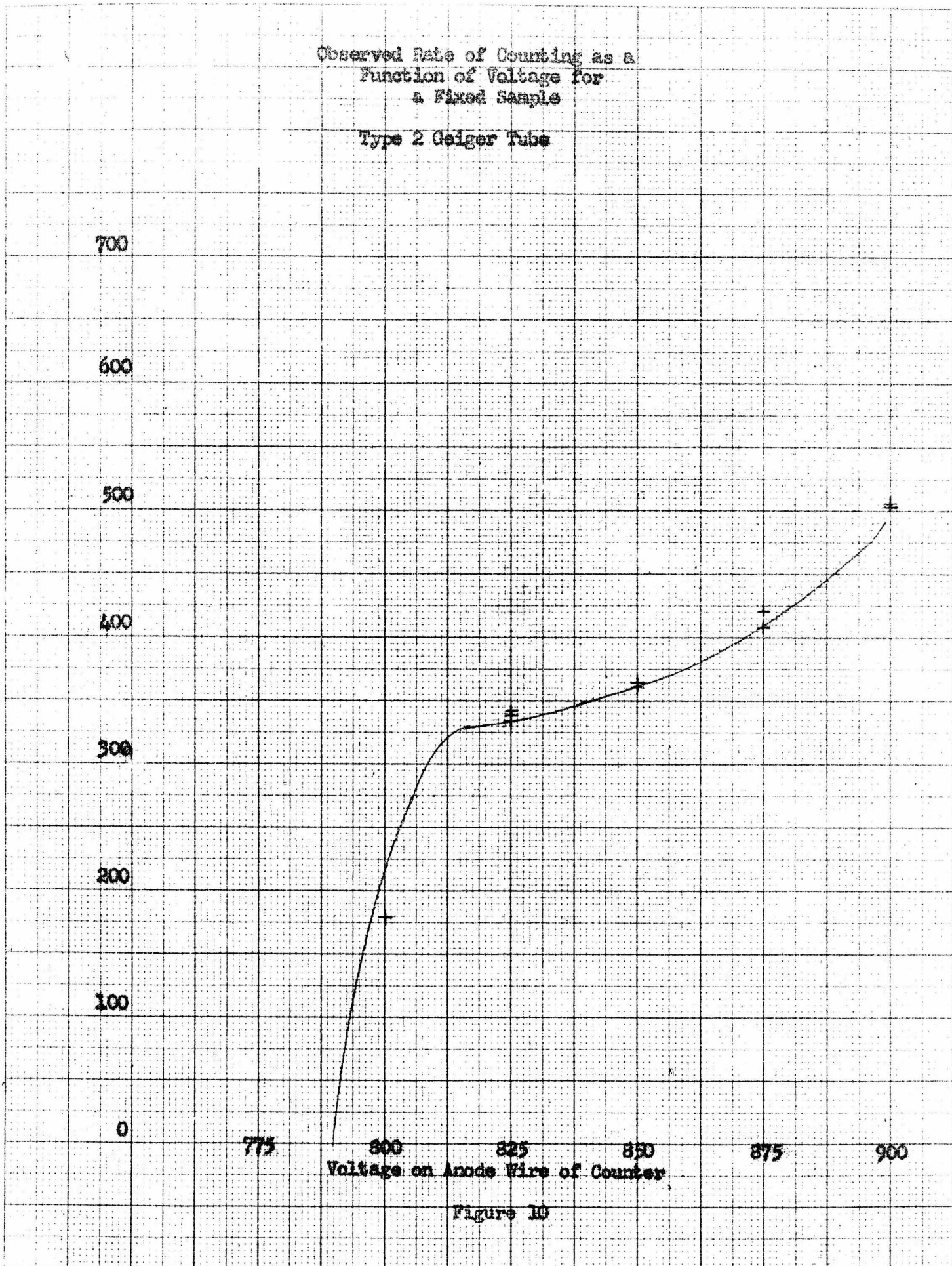


Figure 10

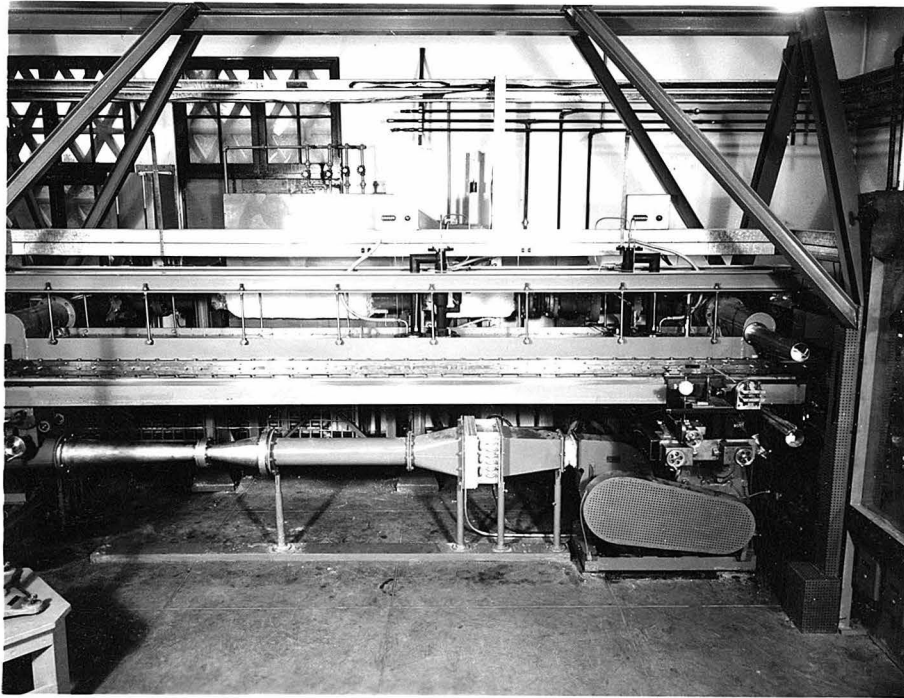


Figure 11

General view of heat transfer apparatus



Figure 12
Traversing gear

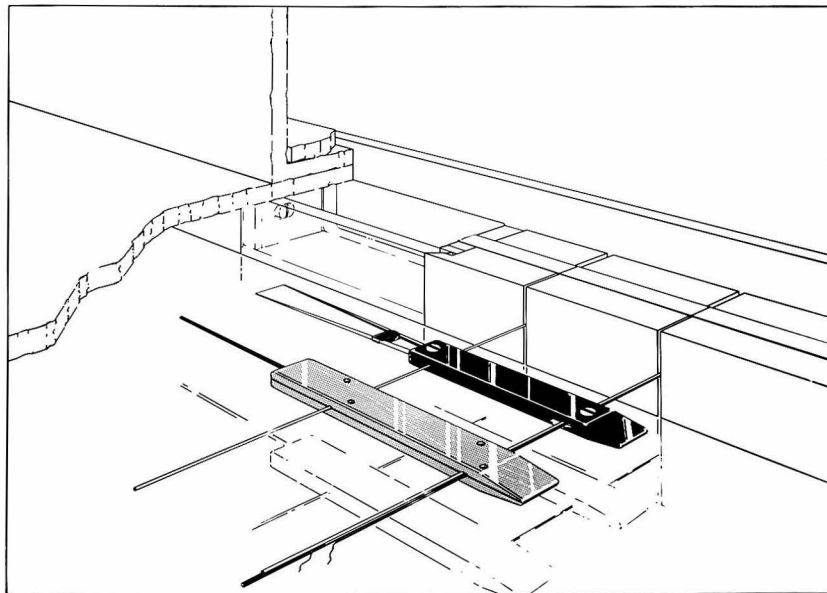


Figure 13

Sampling tube and hot wire anemometer

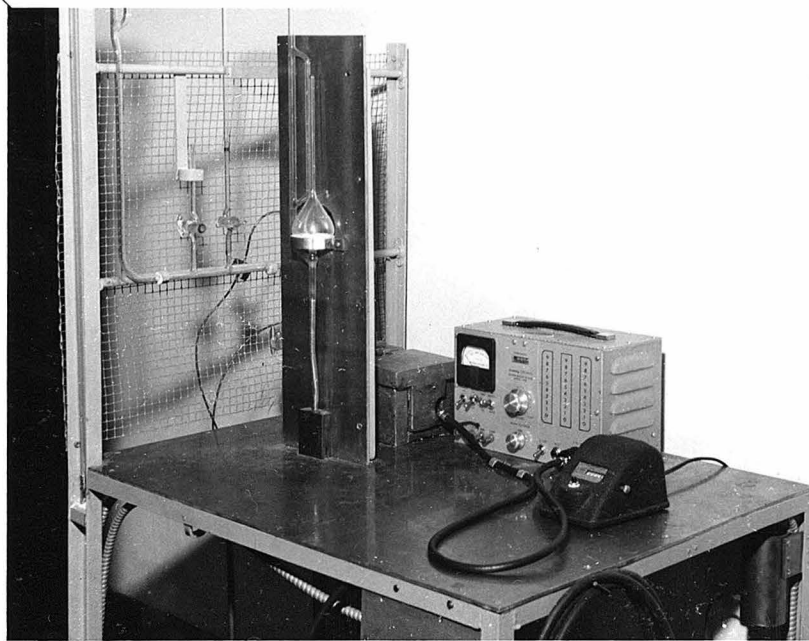


Figure 14
Portable analysis unit

Observed Rate of Counting as a
Function of Voltage for
a Fixed Sample

Type 3 Geiger Tube

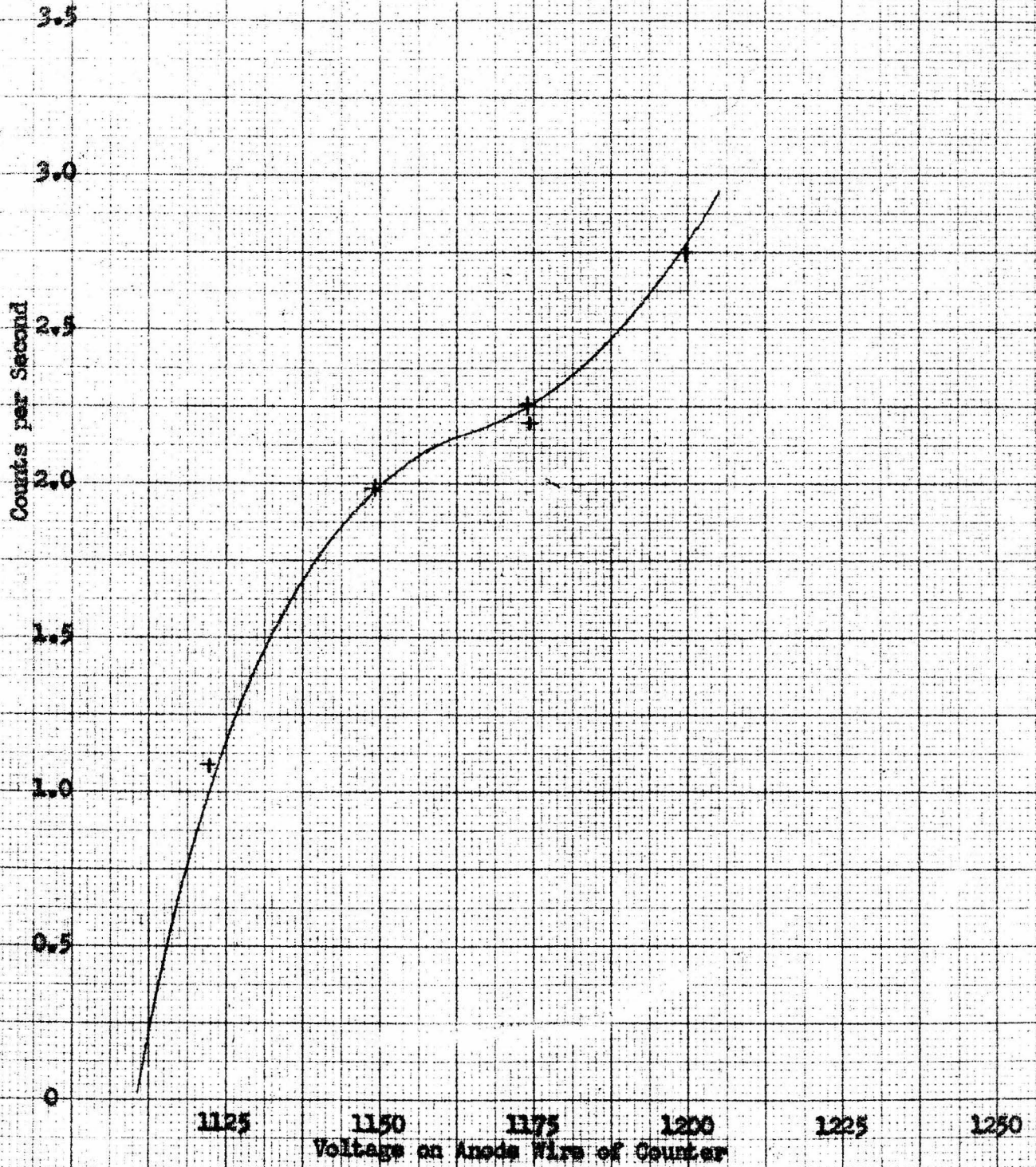


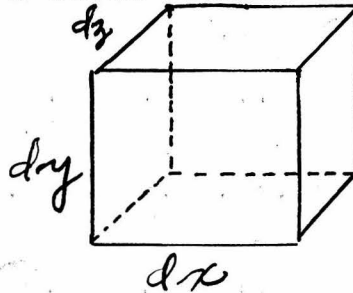
Figure 15

APPENDIX I

General Differential Equations of Thermal Transfer

Equations are derived in this section for two-dimensional thermal transfer in Cartesian coordinates and cylindrical coordinates.

Let us consider a small element of fluid as shown below.



The rate at which energy enters the y-z face of the cube due to eddy and molecular conduction is

$$c_p \sigma (K + \epsilon_c)_x \left(\frac{\partial t}{\partial x} \right) dy dz$$

The rate at which energy enters this face of the cube due to motion of the fluid is

$$u_x (H \sigma) dy dz$$

By means of a similar consideration of energy transfer through the other faces of the cube, the rate of accumulation of energy within the element is found to be

$$\left(\frac{\partial \sigma H}{\partial \theta} \right) dx dy dz$$

In spite of the fact that the specific volume of

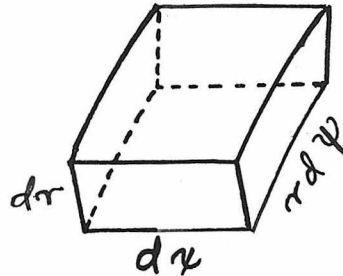
the fluid may change with conditions, the rate of energy accumulation is also equal to

$$c_p \sigma \left[\frac{\partial [K + \epsilon_{cx}] \frac{\partial t}{\partial x}}{\partial x} + \frac{\partial [K + \epsilon_{cy}] \frac{\partial t}{\partial y}}{\partial y} - \frac{\partial (u_x H \sigma)}{c_p \sigma \partial x} - \frac{\partial (u_y H \sigma)}{c_p \sigma \partial y} \right] dx dy dz$$

Combination of these expressions yields the result

$$c_p \sigma \left\{ \frac{\partial [K + \epsilon_{cx}] \frac{\partial t}{\partial x}}{\partial x} + \frac{\partial [K + \epsilon_{cy}] \frac{\partial t}{\partial y}}{\partial y} \right\} - \frac{\partial (u_x H \sigma)}{\partial x} - \frac{\partial (u_y H \sigma)}{\partial y} = \frac{\partial \sigma H}{\partial \theta}$$

In cylindrical coordinates, we have the element of fluid drawn below.



The rate of conduction of energy into the cube through the face in the $r-\psi$ plane is

$$c_p \sigma (K + \epsilon_c)_x \left(\frac{\partial t}{\partial x} \right) r dr d\psi$$

The rate of energy movement into the element due to the fluid velocity at this point is

$$u_x (H \sigma) r dr d\psi$$

The rate of energy transfer into the cube by conduction in the r direction (through the $r-x$ face) is

$$c_p \sigma (K + \epsilon_c)_r \left(\frac{\partial t}{\partial r} \right) dx r d\psi$$

And the movement into the element by means of the fluid's

velocity in the r direction is equal to

$$u_r (H\sigma) r d\psi dx$$

Combining all these expressions, we find the general differential equation to be

$$c_p \sigma \left\{ \frac{\partial [r(k+\epsilon_c) r \frac{\partial t}{\partial r}]}{\partial r} + r \frac{\partial [(k+\epsilon_c) x \frac{\partial t}{\partial x}]}{\partial x} \right\} - \frac{\partial (rH\sigma u_r)}{\partial r} - \frac{\partial (rH\sigma u_x)}{\partial x} = r \frac{\partial H\sigma}{\partial \theta}$$

Let us assume the fluid to be incompressible, with enthalpy independent of pressure, and with C_p independent of temperature. Our equation for rectangular coordinates then takes the form

$$\frac{\partial [(k+\epsilon_c) x \frac{\partial t}{\partial x}]}{\partial x} + \frac{\partial [(k+\epsilon_c) y \frac{\partial t}{\partial y}]}{\partial y} - u_y \frac{\partial t}{\partial y} - u_x \frac{\partial t}{\partial x} = \frac{\partial t}{\partial \theta}$$

And in cylindrical coordinates, the result is

$$\frac{\partial [r(k+\epsilon_c) r \frac{\partial t}{\partial r}]}{\partial r} + r \frac{\partial [(k+\epsilon_c) x \frac{\partial t}{\partial x}]}{\partial x} - \frac{\partial (r u_r t)}{\partial r} - u_x \frac{\partial t}{\partial x} = r \frac{\partial t}{\partial \theta}$$

When this equation is applied under steady state conditions

(that is, $\frac{\partial t}{\partial \theta} = 0$), where velocity in the radial direction may be neglected, as inside tubes or in most axially symmetrical jets, equation (35) of Part I is obtained. If the further simplification that the eddy conductivity in the x , or axial direction is applied, equations (17) and (36) of Part I, which are identical, result.

Propositions submitted by Rodman Jenkins

.D. Oral Examination, August 26, 1949, 1:00 P. M., Crellin Conference Room.

Committee: Professors Sage (Chairman), Lacey, Lucas, Pauling, Schomaker, Yost.

Chemical Engineering

1. The effect of pressure on the rate of homogeneous gas phase chemical reactions may be determined by performing the reaction in a constant volume type pressure-volume-temperature cell. The reaction rate could be found from measurement of the pressure in the bomb as a function of time with the aid of supplementary pressure-volume-temperature data on the system in question.

2. The application of Eyring's theory of viscous flow to the correlation of the viscosities of fluids at high pressures, particularly near the critical region, should be investigated. Thermodynamic data on such fluids may be used to calculate values of the internal pressures. This may be combined with equations of Ewell and Eyring, (1), to find values of viscosity.

3. A fundamental study of the drying of granular solids may be performed by passing an air stream over a bed of wet, regularly packed, spheres.

4. By using a eutectic mixture of sodium nitrate, sodium nitrite, and potassium nitrate as a medium for temperature control, a pressure-volume-temperature cell for use at temperatures up to 1000°F could be constructed.

Chemistry

6. The continuous transition between metallic and non-metallic liquids may be illustrated by an experimental study of the viscosity of solutions of alkali metals in liquid ammonia.

7. Pure specimens of refractory metals, such as titanium, may be prepared by the reaction of a volatile halide (if such exists) in the gas phase with an alkali metal vapor.

8. Relative concentrations of radioactive materials emitting β and γ rays may be measured by means of one or more cylindrical Geiger counters sealed to a gas sample chamber.

Mechanical Engineering

9. Stress analysis of complex parts may be accomplished by solution of appropriate finite difference equations with punch card computing machinery.

10. At high values of the Prandtl number, the variation of local heat transfer coefficients with the Prandtl number should be the same for flow in tubes and for flow transverse to cylinders and other shapes.

Reference

1. R. H. Ewell and H. Eyring, J. Chem. Phys., 5, 726 (1937).